NUSC Technical Report 8827
1 February 1991

AD-A234 478

Complex Envelope Properties, Interpretation, Filtering, and Evaluation

Albert H. Nuttall
Surface ASW Directorate

DTIC
ELECTE
APR 03 1991
S B D

Naval Underwater Systems Center
Newport, Rhode Island • New London, Connecticut

Approved for public release; distribution is unlimited.

PREFACE

This research was conducted under NUSC Project No. A70272, Subproject No. RR0000-N01, **Selected Statistical Problems in Acoustic Signal Processing**, Principal Investigator Dr. Albert H. Nuttall (Code 304). This technical report was prepared with funds provided by the NUSC In-House Independent Research and Independent Exploratory Development Program, sponsored by the Office of the Chief of Naval Research. Also, this report was funded under NUSC Project No. X59458, Principal Investigator Louis J. Dalsass (Code 3431); this latter task is part of the NUSC SIAS program, Manager Anthony R. Susi (Code 3493). The sponsoring activity is the Space and Naval Warfare Systems Command, Program Manager PMW 153-2.

The technical reviewer for this report was Louis J. Dalsass (Code 3431).

REVIEWED AND APPROVED: 1 FEBRUARY 1991

DAVID DENCE
ATD for Surface Antisubmarine Warfare Directorate

REPORT DOCUMENTATION PAGE

Form Approved
OMB No 0704-0188

Public reporting burden for this collection of information is estimated to average 1 hour per response, including the time for reviewing instructions, searching existing data sources, gathering and maintaining the data needed, and completing and reviewing the collection of information. Send comments regarding this burden estimate or any other aspect of this collection of information, including suggestions for reducing this burden, to Washington Headquarters Services, Directorate for Information Operations and Reports, 1215 Jefferson Davis Highway, Suite 1204, Arlington, VA 22202-4302, and to the Office of Management and Budget, Paperwork Reduction Project (0704-0188), Washington, DC 20503

1. AGENCY USE ONLY (Leave blank)	2. REPORT DATE	3. REPORT TYPE AND DATES COVERED
	1 February 1991	Progress

4. TITLE AND SUBTITLE
Complex Envelope Properties, Interpretation, Filtering, and Evaluation

5. FUNDING NUMBERS
PE 61152N

6. AUTHOR(S)
Albert H. Nuttall

7. PERFORMING ORGANIZATION NAME(S) AND ADDRESS(ES)
Naval Underwater Systems Center
New London Laboratory
New London, CT 06320

8. PERFORMING ORGANIZATION REPORT NUMBER
TR 8827

9. SPONSORING / MONITORING AGENCY NAME(S) AND ADDRESS(ES)
Chief of Naval Research
Office of the Chief of Naval Research
Arlington, VA 22217-5000

10. SPONSORING / MONITORING AGENCY REPORT NUMBER

11. SUPPLEMENTARY NOTES

12a. DISTRIBUTION / AVAILABILITY STATEMENT
Approved for public release;
distribution is unlimited.

12b. DISTRIBUTION CODE

13. ABSTRACT *(Maximum 200 words)*

The complex envelope of a narrowband waveform y(t) typically has logarithmic singularities, due to discontinuities in y(t) or its derivatives, which have little physical significance. The complex envelope also has a very slow decay in time, due to the discontinuous spectrum associated with its very definition; this slow decay can mask weak desired features of the complex envelope. In order to suppress these undesired behaviors of the mathematically defined complex envelope, a filtered version is suggested and investigated in terms of its singularity rejection capability and better decay rate. Finally, numerical computation of the complex envelope, as well as its filtered version, by means of a fast Fourier transform (FFT) is investigated and the effects of aliasing are assessed quantitatively. A program for the latter task, using an FFT collapsing procedure, is furnished in BASIC.

14. SUBJECT TERMS		15. NUMBER OF PAGES
complex envelope	analytic waveform	77
narrowband	Hilbert transform	16. PRICE CODE
modulation	Fourier transform	

17. SECURITY CLASSIFICATION OF REPORT	18. SECURITY CLASSIFICATION OF THIS PAGE	19. SECURITY CLASSIFICATION OF ABSTRACT	20. LIMITATION OF ABSTRACT
UNCLASSIFIED	UNCLASSIFIED	UNCLASSIFIED	SAR

14. SUBJECT TERMS (Cont'd)

filtering
collapsing
quadrature
singularities
fast Fourier transform
single-sided spectrum
extracted modulations

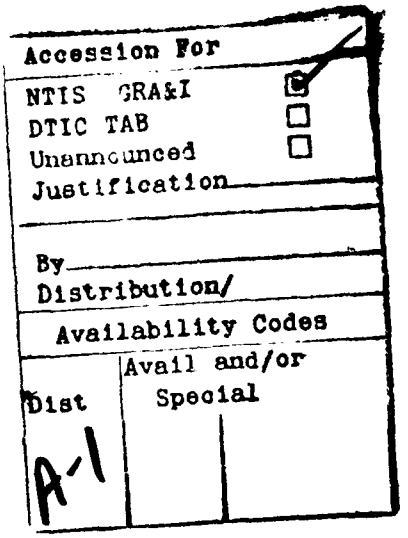

TABLE OF CONTENTS

	Page
LIST OF ILLUSTRATIONS	ii
LIST OF SYMBOLS	iii
INTRODUCTION	1
ANALYTIC WAVEFORM AND COMPLEX ENVELOPE	5
Analytic Waveform	7
Complex Envelope	11
Extracted Amplitude and Phase Modulations	12
Spectrum Y(f) Given	14
Example	17
Singular Behavior	21
General Hilbert Transform Behavior	24
Graphical Results	26
FILTERED COMPLEX ENVELOPE	29
Lowpass Filter	29
Example	31
TRAPEZOIDAL APPROXIMATIONS TO ANALYTIC WAVEFORM, COMPLEX ENVELOPE, AND FILTERED COMPLEX ENVELOPE	39
Complex Envelope	41
Filtered Complex Envelope	42
Graphical Results	44
ALIASING PROPERTIES OF COSINE AND SINE TRANSFORMS	51
General Time Function	51
Causal Complex Time Function	52
Noncausal Real Time Function	53
Causal Real Time Function	53
Aliasing Properties	54
Evaluation by Means of FFTs	60
Displaced Sampling	64
SUMMARY	65
APPENDIX A. DETERMINATION OF CENTER FREQUENCY	67
APPENDIX B. PROGRAM FOR FILTERED COMPLEX ENVELOPE VIA FFT	69
APPENDIX C. CONVOLUTION OF TWO WAVEFORMS	73
REFERENCES	77

LIST OF ILLUSTRATIONS

Figure		Page
1	Spectral Quantities	6
2	Error and Complex Envelope Spectra	10
3	Error e(t) for Various ϕ	28
4	Complex Envelope $\underline{y}(t)$ for Various ϕ	28
5	Filtered Complex Envelope; Desired Terms	36
6	Filtered Complex Envelope; Undesired Terms, $\phi=-\pi/2$	37
7	Filtered Complex Envelope; Undesired Terms, $\phi=0$	37
8	Magnitude of Complex Envelope via FFT, $\phi=-\pi/2$	47
9	Phase of Complex Envelope via FFT, $\phi=-\pi/2$	47
10	Phase of Analytic Waveform via FFT, $\phi=-\pi/2$	48
11	Magnitude of Complex Envelope via FFT, $\phi=0$	48
12	Phase of Complex Envelope via FFT, $\phi=0$	49
13	Magnitude of Filtered Complex Envelope via FFT, $\phi=-\pi/2$	49
14	Phase of Filtered Complex Envelope via FFT, $\phi=-\pi/2$	50

LIST OF SYMBOLS

t	time, (1)
$y(t)$	real waveform, (1)
$a(t)$	imposed amplitude modulation, (1)
$p(t)$	imposed phase modulation, (1)
f_o	carrier frequency, (1)
$z(t)$	imposed complex modulation, (2)
f	frequency, (3)
$Z(f)$	spectrum (Fourier transform) of $z(t)$, (3)
$Y(f)$	spectrum of $y(t)$, (5)
$Y_+(f)$	single-sided spectrum of $y(t)$, (6)
$U(f)$	unit step in f, (6)
$y_+(t)$	analytic waveform, (8)
$N(f)$	negative-frequency function, (9)
$n(t)$	negative-frequency waveform, (10)
Im	imaginary part, (13)
Re	real part, (14)
$y_H(t)$	Hilbert transform of $y(t)$, (15)
$\oplus$	convolution, (15)
$e(t)$	error between Hilbert transform and quadrature, (17)
$E(f)$	error spectrum, (21)
$\underline{y}(t)$	complex envelope, (24)
$\underline{Y}(f)$	spectrum of complex envelope, (26)
$A(t)$	extracted amplitude modulation from $\underline{y}(t)$, (29), (42)
$P(t)$	extracted phase modulation from $\underline{y}(t)$, (29), (42)
$q(t)$	quadrature version of (30), (31)

$Q(f)$	spectrum of $q(t)$, (33)
$\mathrm{sgn}(f)$	+1 for $f > 0$, -1 for $f < 0$, (33)
$Y_H(f)$	spectrum of Hilbert transform, (33)
f_c	center frequency of $Y_+(f)$, (40), appendix A
α	exponential parameter, (45)
ϕ	phase parameter, (45)
ω	radian frequency $2\pi f$, (46)
ω_o	$2\pi f_o$, (46)
c	$\alpha - i\omega_o$, (46)
$E_1(z)$	exponential integral, (53), (64)
t_o	time of discontinuity, (77)
D	size of discontinuity, (77)
$H(f)$	lowpass filter, (83)
f_1	cutoff frequency, (83)
$G(f)$	filtered complex envelope spectrum, (84)
$g(t)$	filtered complex envelope, (85), (86)
$h(t)$	impulse response of lowpass filter $H(f)$, (85)
$g_d(t)$	desired component of filtered complex envelope, (86)
$g_u(t)$	undesired component of filtered complex envelope, (86)
$E(z)$	auxiliary exponential integral, (87)
u_n, v_n	auxiliary variables, (90), (91)
Δ	frequency increment, (102)
$\tilde{y}_+(t)$	approximation to analytic waveform $y_+(t)$, (102)
$\{\varepsilon_n\}$	sequence which is ½ for $n = 0$, 1 for $n \geq 1$, (102)
N	number of time points, size of FFT, (104), (106)
$\{z_n\}$	collapsed sequence, (105), (118)
$\tilde{\underline{y}}(t)$	approximation to complex envelope $\underline{y}(t)$, (109)

α	shift of frequency samples, (114)
$\tilde{g}_\alpha(t)$	approximation to filtered complex envelope, (114)
$\tilde{A}(t)$	magnitude of $\tilde{y}(t)$, figure 8
$\tilde{P}(t)$	phase of $\tilde{y}(t)$, figure 9
$y_e(t)$	even part of y(t), (121)
$y_o(t)$	odd part of y(t), (121)
$y_1(t)$	approximation to (119), (131)
$y_{2c}(t)$	approximation to (125), (134)
$y_{2s}(t)$	approximation to (126), (136)
$y_3(t)$	approximation to (127), (138)
$y_{4c}(t)$	approximation to (129), (141)
$y_{4s}(t)$	approximation to (130), (142)
$z_1(t)$	Fourier transform of single-sided $Y_r(f)$, (149)
$z_2(t)$	Fourier transform of single-sided $Y_i(f)$, (153)
β	displaced sampling time, (155)
FFT	fast Fourier transform

TR 8827

COMPLEX ENVELOPE PROPERTIES, INTERPRETATION, FILTERING, AND EVALUATION

INTRODUCTION

When a narrowband input excites a passband filter, the output time waveform y(t) is a narrowband process with low-frequency amplitude- and/or phase-modulations. The evaluation of this output process y(t) can entail an extreme amount of calculations if the detailed behavior of the higher-frequency carrier is tracked. A much better procedure in this case is to concentrate instead on determination of the low-frequency complex envelope of the narrowband output process y(t) and to state the carrier frequency associated with it. Then, the detailed nature of the output can be found at any time points of interest if desired, although, often, the complex envelope itself is the quantity of interest.

The complex envelope of output y(t) is determined from its spectrum (Fourier transform) Y(f) by suppressing the negative frequencies, down-shifting by the carrier frequency, and Fourier transforming back into the time domain. For a complicated input spectrum and/or filter transfer function with slowly decaying spectral skirts, these calculations can encounter a large number of data points and require large-size fast Fourier transforms (FFTs) for their direct realization. In this case, the use of collapsing or pre-aliasing [1; pages 4 - 5] can be fruitfully employed, thereby keeping storage and FFT sizes small, without any loss of accuracy. This procedure will be employed here.

As will be seen, when the complex envelope is re-applied to the one-sided carrier term and the real part taken, the exact narrowband waveform y(t) is recovered. However, if the complex envelope itself is the quantity of interest, it has some undesirable features. The first problem is related to the fact that if waveform y(t) has any discontinuities in time, its Hilbert transform contains logarithmic infinities, which show up in the complex envelope. The second problem is generated by the operation of truncating the negative frequencies in spectrum Y(f); this creates a discontinuous spectrum which leads to a very slow decay in time of the magnitude of the complex envelope. Since numerical calculation of the complex envelope is necessarily accomplished by sampling spectrum Y(f) in frequency f and performing FFTs, this slow time decay leads to significant aliasing and distortion in the time domain of the computed quantities.

Because these features in the mathematically defined complex envelope are very undesirable, there is a need to define and investigate a modified complex envelope which more nearly corresponds to physical interpretation and utility. The time discontinuities in y(t) show up in Y(f) as a 1/f decay for large frequencies, whereas the truncation of the negative frequencies of Y(f) shows up as a discontinuity directly in f. Both of these spectral properties can be controlled by filtering the truncated spectral quantity, prior to transforming back to the time domain. We will address this filtered complex envelope and its efficient evaluation in this report.

When the waveform y(t) is real and/or causal, its spectrum Y(f) possesses special properties which enable alternative methods of calculation. Thus, it sometimes suffices to have only the real (or imaginary) part of Y(f) and to employ a cosine (or sine) transform, rather than a complex exponential transform. The aliasing properties of these special transforms, when implemented by means of FFTs, will also be addressed here.

ANALYTIC WAVEFORM AND COMPLEX ENVELOPE

Waveform $y(t)$ is real with amplitude modulation $a(t)$ and phase modulation $p(t)$ applied on given carrier frequency f_o; however, $y(t)$ need not be narrowband. That is,

$$y(t) = a(t) \cos[2\pi f_o t + p(t)] = \mathrm{Re}\{z(t) \exp(i2\pi f_o t)\} , \qquad (1)$$

where complex lowpass waveform

$$z(t) \equiv a(t) \exp[ip(t)] \qquad (2)$$

will be called the imposed modulation. The corresponding spectrum of imposed modulation $z(t)$ is

$$Z(f) = \int dt \exp(-i2\pi ft) z(t) . \qquad (3)$$

(Integrals without limits are from $-\infty$ to $+\infty$.) The magnitude of spectrum $Z(f)$ is depicted in figure 1; it is generally concentrated near frequency $f = 0$. The graininess of the curves here is due to plotter quantization, not function discontinuities.

From (1), since waveform

$$y(t) = \frac{1}{2} z(t) \exp(i2\pi f_o t) + \frac{1}{2} z^*(t) \exp(-i2\pi f_o t) , \qquad (4)$$

its spectrum can be expressed as (see figure 1)

$$Y(f) = \frac{1}{2} Z(f-f_o) + \frac{1}{2} Z^*(-f-f_o) \; ; \quad Y(-f) = Y^*(f) . \qquad (5)$$

It will be assumed here that $y(t)$ has no dc component; that is, $Y(f)$ contains no impulse at $f = 0$.

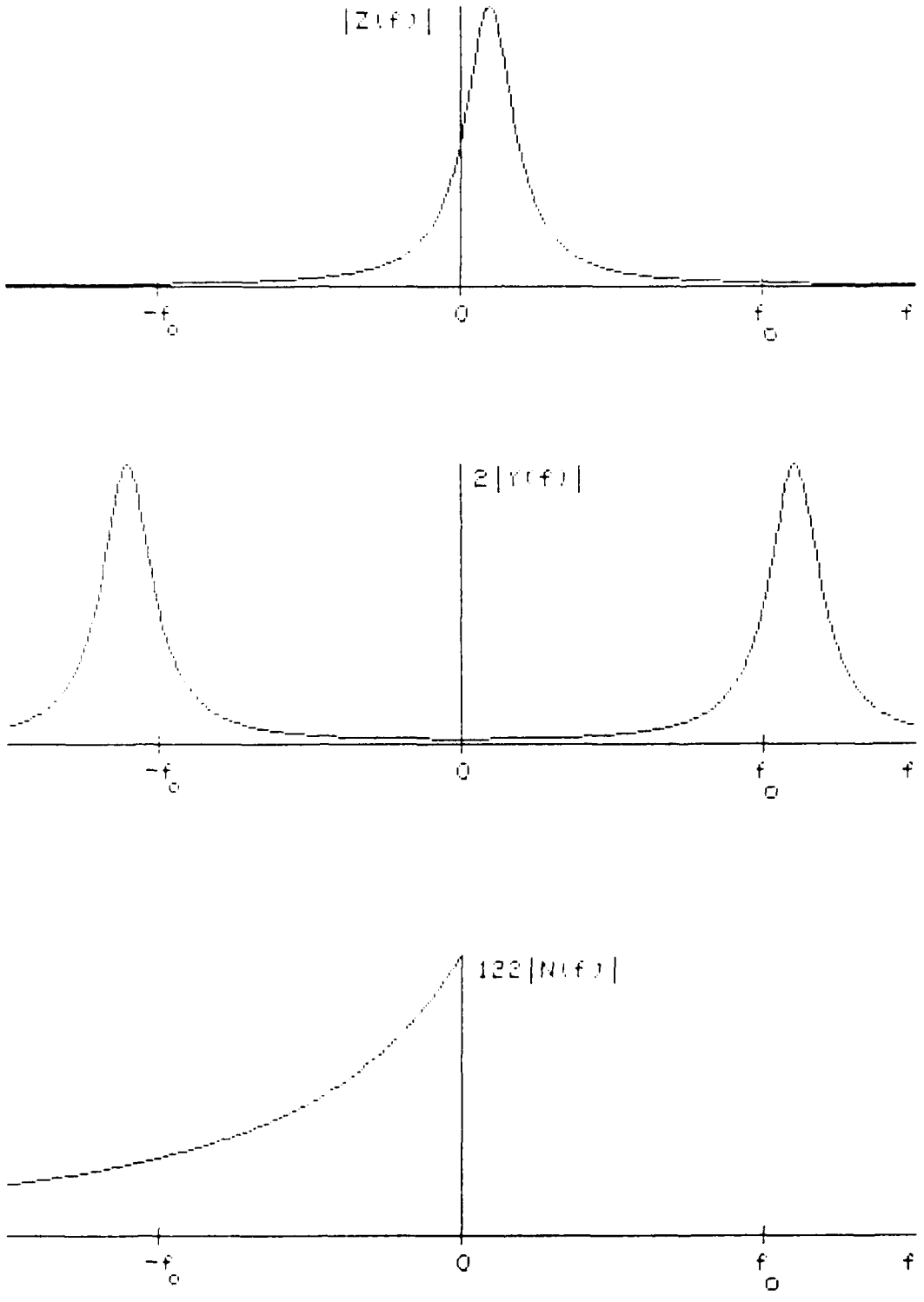

Figure 1. Spectral Quantities

ANALYTIC WAVEFORM

The single-sided (positive) frequency spectrum is defined as

$$Y_+(f) = 2\,U(f)\,Y(f) = U(f)\,Z(f-f_o) + U(f)\,Z^*(-f-f_o) = \quad (6)$$

$$= Z(f-f_o) - U(-f)\,Z(f-f_o) + U(f)\,Z^*(-f-f_o) \quad \text{for all } f\ . \quad (7)$$

Here, $U(x)$ is the unit step function; that is, $U(x)$ is 1 for $x > 0$ and $U(x)$ is 0 for $x < 0$. The analytic waveform corresponding to $y(t)$ is then given by Fourier transform

$$y_+(t) = \int df\ \exp(i2\pi ft)\ Y_+(f)\ . \quad (8)$$

In order to further develop (8), we define a single-sided (negative) frequency function

$$N(f) = U(-f)\,Z(f-f_o) = \begin{cases} 0 & \text{for } f > 0 \\ Z(f-f_o) & \text{for } f < 0 \end{cases}\ , \quad (9)$$

which can be determined directly from the spectrum $Z(f)$ of the imposed modulation $z(t)$ in (2) if f_o is known. The magnitude of $N(f)$, scaled to peak value 1, is sketched in figure 1; it is small if f_o is large, and is peaked near $f = 0$. The complex time function corresponding to (negative frequency) function $N(f)$ is

$$n(t) = \int df\ \exp(i2\pi ft)\ N(f) = \int_{-\infty}^{0} df\ \exp(i2\pi ft)\ Z(f-f_o)\ . \quad (10)$$

With the help of (9) and (10), the single-sided spectrum $Y_+(f)$ in (7) can now be expressed as

$$Y_+(f) = Z(f-f_o) - N(f) + N^*(-f) \ , \tag{11}$$

with corresponding analytic waveform (8)

$$y_+(t) = \exp(i2\pi f_o t)\ z(t) - n(t) + n^*(t) = \tag{12}$$

$$= \exp(i2\pi f_o t)\ z(t) - i\ 2\ \mathrm{Im}\{n(t)\} \ . \tag{13}$$

That is, the analytic waveform is composed of two parts, the first of which is what we would typically desire, namely the imposed modulation (2) shifted up in frequency by f_o. The second term in (13), which is totally imaginary, is usually undesired; it can be seen from (10) and $|N(f)|$ in figure 1 to be generally rather small. There also follows immediately, from (13) and (2), the expected result

$$\mathrm{Re}\{y_+(t)\} = a(t)\ \cos[2\pi f_o t + p(t)] = y(t) \ . \tag{14}$$

Since analytic waveform $y_+(t)$ can also be expressed as

$$y_+(t) = y(t) + i\ y_H(t) = y(t) + i\ y(t) \circledast \frac{1}{\pi t} = y(t) + i\int du\ \frac{y(u)}{\pi(t-u)}, \tag{15}$$

where $y_H(t)$ is the Hilbert transform of $y(t)$ and $\circledast$ denotes convolution, (13) and (2) yield

$$y_H(t) = a(t)\ \sin[2\pi f_o t + p(t)] - 2\ \mathrm{Im}\{n(t)\} \ . \tag{16}$$

If we define (real) error waveform $e(t)$ as the difference between the Hilbert transform of (1) and the quadrature version of original waveform (1), we have

$$e(t) \equiv y_H(t) - a(t)\,\sin[2\pi f_o t + p(t)] = \tag{17}$$

$$= -\,2\,\mathrm{Im}\{n(t)\} = i\,[n(t) - n^*(t)] = \tag{18}$$

$$= -\,2\,\mathrm{Im}\int_{-\infty}^{0} df\,\exp(i2\pi ft)\,Z(f-f_o) = \tag{19}$$

$$= -\,2\,\mathrm{Im}\left\{\exp(i2\pi f_o t)\int_{-\infty}^{-f_o} df\,\exp(i2\pi ft)\,Z(f)\right\}, \tag{20}$$

where we used (16) and (10). The error spectrum is, from (18) and (9),

$$E(f) = i\,[N(f) - N^*(-f)] = \tag{21}$$

$$= \begin{cases} -i\,Z^*(-f-f_o) & \text{for } f > 0 \\ i\,Z(f-f_o) & \text{for } f < 0 \end{cases}. \tag{22}$$

Then, $E(-f) = E^*(f)$. The magnitude of $E(f)$ is displayed in figure 2; it is generally small and centered about $f = 0$.

The total energy in real error waveform $e(t)$ is

$$\int dt\,[e(t)]^2 = \int df\,|E(f)|^2 =$$

$$= \int df\,\left[N(f) - N^*(-f)\right]\left[N^*(f) - N(-f)\right] =$$

$$= \int df\,\left[|N(f)|^2 + |N(-f)|^2\right] = 2\int df\,|N(f)|^2 =$$

$$= 2\int_{-\infty}^{0} df\,|Z(f-f_o)|^2 = 2\int_{-\infty}^{-f_o} df\,|Z(f)|^2, \tag{23}$$

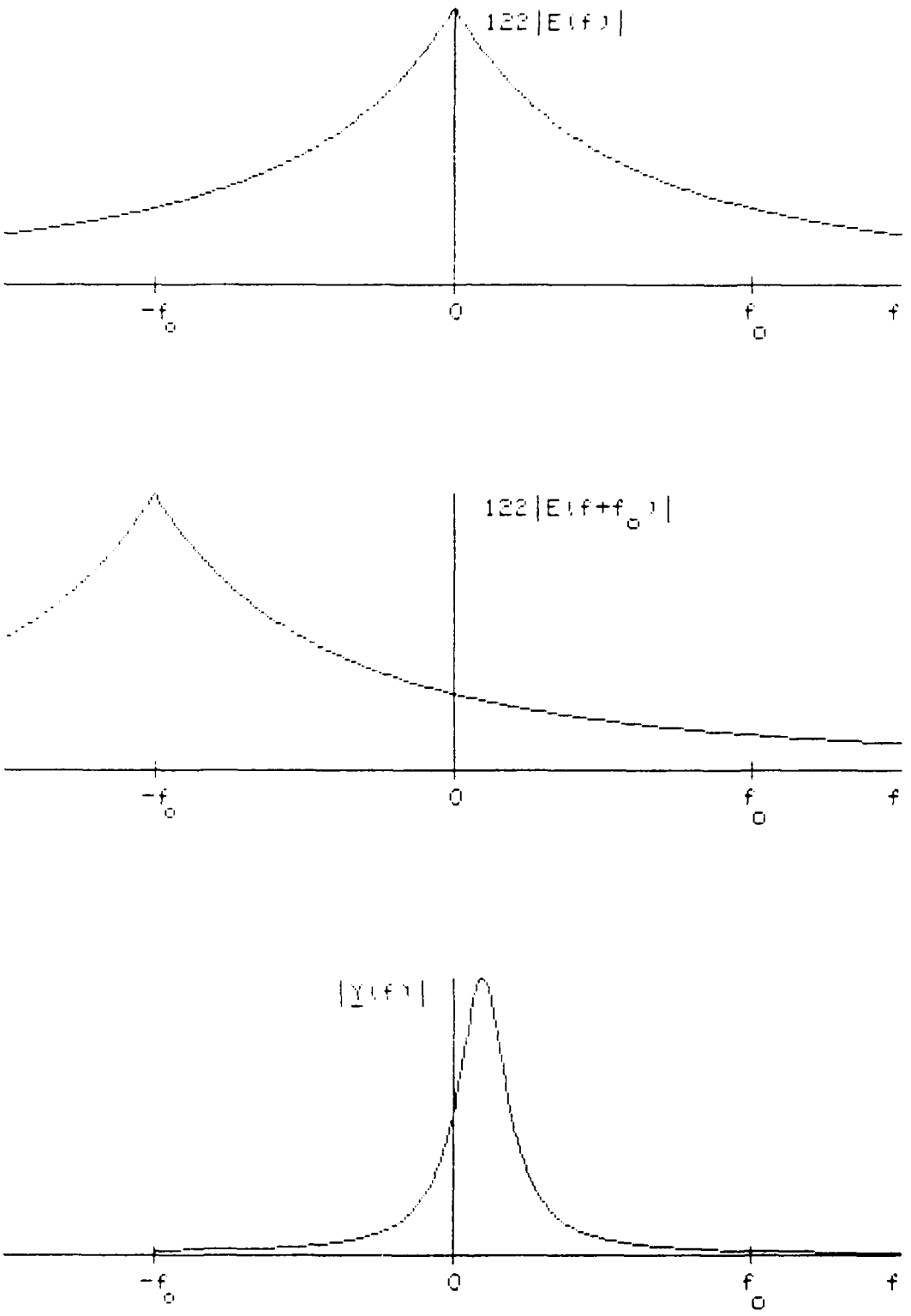

Figure 2. Error and Complex Envelope Spectra

where we used (21), the single-sided behavior of N(f), and (9). This is just twice the energy in the spectrum Z(f) of imposed modulation z(t) below frequency $-f_o$; inspection of figure 1 reveals that this quantity will usually be small.

COMPLEX ENVELOPE

The complex envelope $\underline{y}(t)$ of waveform y(t) is the frequency down-shifted version of analytic waveform $y_+(t)$:

$$\underline{y}(t) \equiv y_+(t) \exp(-i2\pi f_o t) = \tag{24}$$

$$= z(t) + i\, e(t) \exp(-i2\pi f_o t) , \tag{25}$$

where we used (13) and (18) and chose to downshift by f_o Hertz, the known carrier frequency in (1). Waveforms z(t) and e(t) are lowpass, as may be verified from their spectra in figures 1 and 2. The spectrum of the complex envelope is, from (25),

$$\underline{Y}(f) = Z(f) + i\, E(f+f_o) . \tag{26}$$

Equations (25) and (26) show that the complex envelope and its spectrum are each composed of a desired component and an error term.

The magnitudes of the complex envelope spectrum $\underline{Y}(f)$ and its error component are displayed in figure 2; $\underline{Y}(f)$ is discontinuous at $f = -f_o$ but has zero slope as $f \to -f_o$, whether from above or below. The left tail of Z(f) and shifted error spectrum, $i\, E(f+f_o)$, interact so as to yield $\underline{Y}(f) = 0$ for $f < -f_o$; this is most easily seen from a combination of (24) and (6), namely

$$\underline{Y}(f) = Y_{+}(f+f_o) = 2\ U(f+f_o)\ Y(f+f_o) = \tag{27}$$

$$= U(f+f_o)\ [Z(f) + Z^{*}(-f-2f_o)]\ . \tag{28}$$

The results for the error spectrum and energy in (22) and (23), respectively, were originally derived by Nuttall [2]; however, we have augmented those results here, to give detailed expressions for the error and complex envelope waveforms and spectra. There are no approximations in any of the above relations; they apply to waveforms with arbitrary spectra, whether carrier frequency f_o is large or small.

EXTRACTED AMPLITUDE AND PHASE MODULATIONS

It is important and useful to also make the following observations relative to the amplitude and phase modulations that can be extracted from the complex envelope $\underline{y}(t)$. Define

$$A(t) = |\underline{y}(t)|\ , \qquad P(t) = \arg\{\underline{y}(t)\}\ . \tag{29}$$

Then, from (14) and (24), the original waveform can be expressed in terms of these extracted amplitude and phase modulations as

$$y(t) = \mathrm{Re}\{\underline{y}(t)\ \exp(i2\pi f_o t)\} = A(t)\ \cos[2\pi f_o t + P(t)]\ . \tag{30}$$

However, complex-envelope modulations A(t) and P(t) in (29) and (30) are not generally equal to imposed modulations a(t) and p(t) in (1), as may be seen by reference to (25). Namely, complex envelope $\underline{y}(t)$ is equal to complex lowpass waveform z(t) in (2) only if error e(t) is zero. But the energy in waveform e(t), as

given by (23), is zero only if imposed spectrum Z(f) in (3) is zero for $f < -f_o$. When Z(f) is not zero for $f < -f_o$, complex-envelope modulations A(t) and P(t) do not agree with imposed modulations a(t) and p(t), <u>despite</u> the ability to write y(t) in the two similar real forms (1) and (30) involving an amplitude- and phase-modulated cosine with the same f_o.

Another interesting property of form (30) is that its quadrature version is <u>identically</u> the Hilbert transform of y(t). This is in contrast with the quadrature version of (1) involving imposed modulations a(t) and p(t); see (17) - (20). To prove this claim, observe that the quadrature version of the last term of (30) is, using (29),

$$q(t) \equiv A(t)\ \sin[2\pi f_o t + P(t)] = \tag{31}$$

$$= \frac{1}{i2}\ [A(t)\ \exp(iP(t) + i2\pi f_o t) - A(t)\ \exp(-iP(t) - i2\pi f_o t)] =$$

$$= \frac{1}{i2}[\underline{y}(t)\ \exp(i2\pi f_o t) - \underline{y}^*(t)\ \exp(-i2\pi f_o t)]\ . \tag{32}$$

The spectrum of this waveform is

$$Q(f) = \frac{1}{i2}\left[\underline{Y}(f-f_o) - \underline{Y}^*(-f-f_o)\right] = -i[U(f)\ Y(f) - U(-f)\ Y^*(-f)] =$$

$$= \left\{\begin{matrix} -i\ Y(f) & \text{for } f > 0 \\ i\ Y(f) & \text{for } f < 0 \end{matrix}\right\} = -i\ \text{sgn}(f)\ Y(f) = Y_H(f)\ , \tag{33}$$

where we used (27), the conjugate symmetry of Y(f), sgn(x) = +1 for x > 0 and -1 for x < 0, and (6) in the form

$$Y_+(f) = 2\ U(f)\ Y(f) = [1 + \text{sgn}(f)]\ Y(f) = Y(f) + i\ Y_H(f)\ , \tag{34}$$

the latter result following from (15). Thus, (33) and (31) yield the desired result

$$y_H(t) = \frac{1}{\pi t} \oplus y(t) = q(t) = A(t) \sin[2\pi f_o t + P(t)] \ . \quad (35)$$

This simple connection between (35) and (30) holds in general when modulations A(t) and P(t) are extracted from the complex envelope according to (29); there are no narrowband assumptions required. The more complicated connection between (16) and (1), which is applicable for the imposed modulations, involves an error term; this error is zero if and only if spectrum Z(f) in (3) is zero for $f < -f_o$.

SPECTRUM Y(f) GIVEN

All of the above results have presumed that waveform y(t) in the form (1) was available as the starting point. But there are many problems of interest where spectrum Y(f) is the initial available quantity, rather than y(t). For example, the output spectrum Y(f) of a linear filter L(f) subject to input spectrum X(f) is given by Y(f) = L(f) X(f) and can often be easily and directly computed. In this case, there are no given amplitude and phase modulations a(t) and p(t) as in (1); in fact, there is not even an obvious or unique center frequency for a given spectrum Y(f). Nevertheless, many, but not all, of the relations above hold true under appropriate definitions of the various terms.

Given spectrum $Y(f)$ with conjugate symmetry, $Y(-f) = Y^*(f)$, we begin with its corresponding real waveform

$$y(t) = \int df\ \exp(i2\pi ft)\ Y(f)\ . \tag{36}$$

The Hilbert transform of $y(t)$ and its spectrum are given by

$$y_H(t) = \frac{1}{\pi t} \circledast y(t)\ , \quad Y_H(f) = -i\ \mathrm{sgn}(f)\ Y(f)\ . \tag{37}$$

The single-sided spectrum and analytic waveform are, respectively

$$Y_+(f) = 2\ U(f)\ Y(f) = [1 + \mathrm{sgn}(f)]\ Y(f) = Y(f) + i\ Y_H(f)\ , \tag{38}$$

$$y_+(t) = 2 \int_0^\infty df\ \exp(i2\pi ft)\ Y(f) = y(t) + i\ y_H(t)\ . \tag{39}$$

Up to this point, all the functions are unique and nothing has changed. However, we now have to choose a "center frequency" f_c of $Y_+(f)$, since none has been specified; this (somewhat arbitrary) selection process of f_c is addressed in appendix A, to which the reader is referred at this point. Hence, we take f_c as given and define lowpass spectrum

$$\underline{Y}(f) = Y_+(f+f_c) = 2\ U(f+f_c)\ Y(f+f_c)\ . \tag{40}$$

The corresponding complex envelope is

$$\underline{y}(t) = y_+(t)\ \exp(-i2\pi f_c t)\ . \tag{41}$$

We define the complex-envelope amplitude and phase modulations as in (29):

$$A(t) = |\underline{y}(t)|\ , \quad P(t) = \arg\{\underline{y}(t)\} = \arg\{y_+(t)\} - 2\pi f_c t\ . \tag{42}$$

Then, from (39), (41), and (42), we have

$$y(t) = \mathrm{Re}\{y_+(t)\} = \mathrm{Re}\{\underline{y}(t)\ \exp(i2\pi f_c t)\} = A(t)\ \cos[2\pi f_c t + P(t)]. \tag{43}$$

Now when we define the quadrature version of the right-hand side of (43) in a manner similar to (31), but now employing f_c instead of (unspecified) f_o, the same type of manipulations as in (31) - (35) yield relations identical to those given above:

$$Q(f) = Y_H(f)\ ,\quad y_H(t) = q(t) = A(t)\ \sin[2\pi f_c t + P(t)]\ . \tag{44}$$

Because the choice of center frequency f_c of single-sided spectrum $Y_+(f)$ is somewhat arbitrary (see appendix A), this makes complex envelope $\underline{y}(t)$ and its extracted phase $P(t)$ somewhat arbitrary. However, the argument, $2\pi f_c t + P(t) = \arg\{y_+(t)\}$, of (43) and (44) is <u>not</u> arbitrary, as seen directly from (41) and the uniqueness of $y_+(t)$ in (39). Furthermore, extracted amplitude modulation $A(t)$ in (42) has no arbitrariness since it is given alternatively by $|y_+(t)|$, according to (41).

Since $A(t)$ and $P(t)$ are lowpass functions, we can compute them at relatively coarse increments in time t. Then, if we want to observe the fine detail of $y(t)$, as given by (43), we can interpolate between these values of $A(t)$ and $P(t)$ and then compute the cosine in (43) at whatever t values are of interest. This practical numerical approach will reduce the number of computations of $A(t)$ and $P(t)$ required; in fact, in many applications, $A(t)$ and $P(t)$ will themselves be the desired output quantities of interest, rather than narrowband waveform $y(t)$ with all its unimportant high-frequency detail.

EXAMPLE

Consider the fundamental building block of systems with rational transfer functions, namely

$$y(t) = U(t)\exp(-\alpha t)\cos(2\pi f_o t + \phi) , \quad \alpha > 0 , \quad f_o > 0 , \tag{45}$$

where U(t) is the unit step in time t. Let

$$\omega = 2\pi f , \quad \omega_o = 2\pi f_o , \quad c = \alpha - i\omega_o . \tag{46}$$

Then, from (1) and (2), the imposed modulations are

$$a(t) = U(t)\exp(-\alpha t), \quad p(t) = \phi, \quad z(t) = U(t)\exp(i\phi-\alpha t) , \tag{47}$$

yielding, upon use of (3) and (46), spectrum

$$Z(f) = \frac{\exp(i\phi)}{\alpha + i2\pi f} = \frac{\exp(i\phi)}{\alpha + i\omega} . \tag{48}$$

From (5) and (48), the spectrum of y(t) is

$$Y(f) = \frac{1}{2}\left[\frac{\exp(i\phi)}{\alpha + i(\omega - \omega_o)} + \frac{\exp(-i\phi)}{\alpha + i(\omega + \omega_o)}\right] , \tag{49}$$

and (6) yields single-sided spectrum

$$Y_+(f) = U(f)\left[\frac{\exp(i\phi)}{\alpha + i(\omega - \omega_o)} + \frac{\exp(-i\phi)}{\alpha + i(\omega + \omega_o)}\right] . \tag{50}$$

Now we use (9), (48), and (46) to obtain (negative) spectrum

$$N(f) = U(-f)\,\frac{\exp(i\phi)}{c + i\omega} = \left\{\begin{array}{ll} 0 & \text{for } f > 0 \\ \dfrac{\exp(i\phi)}{c + i\omega} & \text{for } f < 0 \end{array}\right\} . \tag{51}$$

Then, from (10), the corresponding complex time waveform is

$$n(t) = \int_{-\infty}^{0} df\, \exp(i\omega t)\, \frac{\exp(i\phi)}{c + i\omega} = \frac{\exp(i\phi - ct)}{i2\pi} \int_{c-i\infty}^{c} \frac{du}{u} \exp(tu) \ . \quad (52)$$

For $t < 0$, let $x = |t|u = -tu$, to get

$$n(t) = \frac{\exp(i\phi - ct)}{i2\pi} \int_{c|t|-i\infty}^{c|t|} \frac{dx}{x} \exp(-x) = \frac{i}{2\pi} \exp(i\phi - ct)\, E_1(c|t|) \ , \quad (53)$$

where $E_1(z)$ is the exponential integral [3; 5.1.1]. It is important to observe and use the fact that the path of integration in the complex x-plane in (53) remains in the fourth quadrant and never crosses the negative real x-axis [3; under 5.1.6].

Also, for $t > 0$, let $x = -tu$ in (52), to get

$$n(t) = \frac{\exp(i\phi - ct)}{i2\pi} \int_{-ct+i\infty}^{-ct} \frac{dx}{x} \exp(-x) = \frac{i}{2\pi} \exp(i\phi - ct)\, E_1(-ct) \ . \quad (54)$$

Here, the contour of integration remains in the second quadrant of the complex x-plane and again does not cross the negative real x-axis [3; under 5.1.6]. The combination of (53) and (54) now yields complex time waveform

$$n(t) = \frac{i}{2\pi} \exp(i\phi - ct)\, E_1(-ct) \quad \text{for all } t \neq 0 \ . \quad (55)$$

Now, we use (18) to obtain real error waveform

$$e(t) = -\frac{1}{\pi}\,\mathrm{Re}\{\exp(i\phi - ct)\,E_1(-ct)\} \quad \text{for all } t \neq 0\ . \tag{56}$$

(Or we could directly use (20) with (48).) The corresponding error spectrum follows from (22), (48), and (46) as

$$E(f) = \begin{cases} \dfrac{-i\,\exp(-i\phi)}{c^* + i\omega} & \text{for } f > 0 \\ \dfrac{i\,\exp(i\phi)}{c + i\omega} & \text{for } f < 0 \end{cases}\ . \tag{57}$$

From (16), (17), (47), and (56), the Hilbert transform of $y(t)$ is

$$y_H(t) = U(t)\,\exp(-\alpha t)\,\sin(2\pi f_o t + \phi) - \frac{1}{\pi}\,\mathrm{Re}\{\exp(i\phi - ct)\,E_1(-ct)\} \quad \text{for all } t \neq 0. \tag{58}$$

In addition, using (15) and (45), the analytic waveform is

$$y_+(t) = U(t)\,\exp(i\phi - ct) - i\,\frac{1}{\pi}\,\mathrm{Re}\{\exp(i\phi - ct)\,E_1(-ct)\} \quad \text{for all } t \neq 0. \tag{59}$$

The complex envelope follows from (25), (47), and (56) as

$$\underline{y}(t) = U(t)\,\exp(i\phi - \alpha t) - \frac{i}{\pi}\,\exp(-i\omega_o t)\,\mathrm{Re}\{\exp(i\phi - ct)\,E_1(-ct)\} \quad \text{for all } t \neq 0\ . \tag{60}$$

The corresponding spectrum is, from (27) and (50),

$$\underline{Y}(f) = U(f + f_o)\left[\frac{\exp(i\phi)}{\alpha + i\omega} + \frac{\exp(-i\phi)}{\alpha + i(\omega + 2\omega_o)}\right]\ . \tag{61}$$

The extracted amplitude and phase modulations A(t) and P(t) of complex envelope $\underline{y}(t)$ are now available by applying (42) to (60). Since the first term, by itself, in (60) has the imposed amplitude and phase modulations a(t) and p(t) as specified in (47), A(t) cannot possibly equal a(t), nor can P(t) equal p(t). This example is an illustration of the general property stated in the sequel to (30). The reason is that spectrum Z(f) in (48) is obviously nonzero for $f < -f_o$.

From (23) and (48), the energy in error waveform e(t) is

$$2 \int_{-\infty}^{-f_o} \frac{df}{\alpha^2 + \omega^2} = \frac{1}{2\alpha}\left[1 - \frac{2}{\pi} \arctan\left(\frac{\omega_o}{\alpha}\right)\right] . \qquad (62)$$

For comparison, the energy in desired component z(t) in complex envelope $\underline{y}(t)$ of (25) is, from (47),

$$\int_{-\infty}^{\infty} dt \, |z(t)|^2 = \frac{1}{2\alpha} . \qquad (63)$$

SINGULAR BEHAVIOR

Since [3; 5.1.11 and footnote on page 228]

$$E_1(z) = - \ln(z) - \gamma + Ein(z) \ , \tag{64}$$

where Ein(z) is entire, the error waveform in (56) has a component

$$- \frac{1}{\pi} \mathrm{Re}\{-\exp(i\phi - ct) \ln(-ct)\} =$$

$$= \frac{1}{\pi} \mathrm{Re}\{\exp(i\phi - ct) [\ln(-c \ \mathrm{sgn}(t)) + \ln|t|] \quad \text{for } t \neq 0 \ , \tag{65}$$

of which the most singular component is

$$\frac{1}{\pi} \ln|t| \exp(-\alpha t) \cos(\omega_o t + \phi) \sim \frac{1}{\pi} \cos(\phi) \ln|t| \text{ as } t \to 0 \ . \tag{66}$$

The only situation for which this logarithmic singularity does not contribute an infinity as $t \to 0$ is when $\phi = - \pi/2$ (or $\pi/2$). That corresponds to the special case in (45) of

$$y(t) = U(t) \exp(-\alpha t) \sin(\omega_o t) \quad \text{for } \phi = - \pi/2 \ , \tag{67}$$

which is zero at $t = 0$; that is, $y(t)$ is continuous for all t. However, even for $\phi = - \pi/2$ in the first term of (66), the product $\ln|t| \sin(\omega_o t)$ has an infinite slope at its zero at $t = 0$, leading possibly to numerical difficulties.

The spectrum Y(f) follows from (49) as

$$Y(f) = \frac{\omega_o}{\alpha^2 + \omega_o^2 + i2\alpha\omega - \omega^2} \quad \text{for } \phi = - \frac{\pi}{2} \ , \tag{68}$$

which decays as ω^{-2} as $\omega \to \pm\infty$; this spectral decay is the key issue for avoiding a logarithmic singularity in $e(t)$, $y_H(t)$, $y_+(t)$, and $\underline{y}(t)$. All values of ϕ other than $\pm\pi/2$ lead to asymptotic decay of $Y(f)$ in (49) according to $-i \cos(\phi)\, \omega^{-1}$, which leads to a logarithmic singularity in the various time functions considered here, including the complex envelope.

Continuing this special case of $\phi = -\pi/2$ in (67) and (68), we find, from (48),

$$Z(f) = \frac{-i}{\alpha + i\omega} , \qquad z(t) = U(t)\ (-i)\ \exp(-\alpha t) \quad \text{for } \phi = -\frac{\pi}{2} . \tag{69}$$

Also, there follows from (56), (58), and (60), respectively, the error, the Hilbert transform, and the complex envelope, as

$$e(t) = -\frac{1}{\pi}\, \mathrm{Im}\{\exp(-ct)\ E_1(-ct)\} , \tag{70}$$

$$y_H(t) = -\,U(t)\ \exp(-\alpha t)\ \cos(\omega_o t) + e(t) , \tag{71}$$

$$\underline{y}(t) = U(t)\ (-i)\ \exp(-\alpha t) + i\ \exp(-i\omega_o t)\ e(t) , \tag{72}$$

all for $\phi = -\pi/2$.

The asymptotic behavior of error $e(t)$ at infinity is available from [3; 5.1.51] as

$$e(t) \sim \frac{\omega_o}{\alpha^2 + \omega_o^2}\ \frac{1}{\pi t} \quad \text{as } t \to \pm\infty \quad \text{for } \phi = -\frac{\pi}{2} . \tag{73}$$

The origin behavior is available from [3; 5.1.11]:

$$e(t) \sim \left\{ \begin{array}{ll} -\frac{1}{\pi}\arctan(\omega_o/\alpha) & \text{as } t \to 0- \\ \\ 1 - \frac{1}{\pi}\arctan(\omega_o/\alpha) & \text{as } t \to 0+ \end{array} \right\} \quad \text{for } \phi = -\frac{\pi}{2} . \qquad (74)$$

Observe that these limits in (74) at $t = \pm 0$ are both finite. Also, note the very slow decay in (73), namely $1/t$, of error $e(t)$ at infinity.

When $\phi \neq \pm\pi/2$, the generalizations to (73) and (74) are [3; 5.1.51 and 5.1.11]

$$e(t) \sim \frac{\alpha \cos\phi - \omega_o \sin\phi}{\alpha^2 + \omega_o^2} \frac{1}{\pi t} \quad \text{as } t \to \pm\infty , \qquad (75)$$

and

$$e(t) \sim \frac{\cos\phi}{\pi} \ln|t| \quad \text{as } t \to 0 . \qquad (76)$$

Now, error $e(t)$ becomes infinite at the origin and decays only as $1/t$ for large t. (If $\tan\phi = \alpha/\omega_o$, then $e(t) = O(t^{-2})$ as $t \to \pm\infty$; this corresponds to $Y(0) = 0$ in (49).)

GENERAL HILBERT TRANSFORM BEHAVIOR

The example of $y(t)$ in (45) (when $\phi \neq \pm\pi/2$) illustrates the general rule that if a time function has a discontinuity of value D at time t_o, then its Hilbert transform behaves as $D/\pi \ln|t-t_o|$ as $t \to t_o$. To derive this result, observe that

$$y(t) \sim V + \tfrac{1}{2}D \operatorname{sgn}(t-t_o) \quad \text{as } t \to t_o \ , \tag{77}$$

when $y(t)$ is discontinuous at t_o. Then, for t near t_o, the Hilbert transform of $y(t)$ is dominated by the components

$$y_H(t) \sim \frac{1}{\pi} \int_{-b}^{-\varepsilon} \frac{du}{u} \left[V + \tfrac{1}{2}D \operatorname{sgn}(t-t_o-u)\right] +$$

$$+ \frac{1}{\pi} \int_{\varepsilon}^{b} \frac{du}{u} \left[V + \tfrac{1}{2}D \operatorname{sgn}(t-t_o-u)\right] \ , \tag{78}$$

where ε is a small positive quantity and the principal value nature of the Hilbert transform integral has been utilized. The integrals involving constant V cancel; also, by breaking the integrals in (78) down into regions where sgn is positive versus negative, and watching whether $t-t_o$ is positive or negative, the terms involving $\ln(\varepsilon)$ cancel, leaving the dominant behavior

$$y_H(t) \sim \frac{D}{\pi} \ln|t-t_o| \quad \text{as } t \to t_o \ . \tag{79}$$

(The example in (66) corresponds to a discontinuity $D = \cos(\phi)$ at $t_o = 0$, as may be seen by referring to (45).) When Hilbert

transform $y_H(t)$ has this logarithmic singularity (79), then so also do $y_+(t)$, $\underline{y}(t)$, and $e(t)$ at the same time location. Thus, the complex envelope corresponding to a discontinuous $y(t)$ has a logarithmic singularity.

An alternative representation for Hilbert transform $y_H(t)$ in (15) is given by

$$y_H(t) = \int df \exp(i2\pi ft) \; (-i) \; \mathrm{sgn}(f) \; Y(f) \; . \qquad (80)$$

If $Y(f)$ decays to zero at $f = \pm\infty$ and if $Y(f)$ is continuous for all real f, then an integration by parts on (80) yields (due to the discontinuity of $\mathrm{sgn}(f)$) the asymptotic decay

$$y_H(t) \sim \frac{Y(0)}{\pi t} \quad \text{as } t \to \pm\infty \; . \qquad (81)$$

(Results (73) and (75) are special cases of (81), when applied to example (49).) The only saving feature of this very slow decay for large t in (81) is that $Y(0)$ may be small relative to its maximum for $f \neq 0$. For example (49), $|Y(f_o)| \cong (2\alpha)^{-1}$ for $\alpha << \omega_o$, which is then much larger than $Y(0) \cong -\sin\phi/\omega_o$. In this narrowband case, the slow decay of (81) will not be overly significant in analytic waveform $y_+(t)$ until t gets rather large. If $Y(0)$ is zero, the dominant behavior is not given by (81), but instead is replaced by a $1/t^2$ dependence, with a magnitude proportional to $Y'(0)$.

GRAPHICAL RESULTS

We now take the example in (45) with parameter values $\alpha = 1$ sec^{-1} and $f_o = 100$ Hz. The error e(t) in (56) is plotted versus time t in figure 3 for three different values of phase ϕ. A time sampling increment Δ_t of .02 msec was used to compute (56), since these error functions are very sharp in t, being concentrated around t = 0 where the waveform y(t) has its discontinuity. The period of the carrier frequency is $1/f_o = 10$ msec; however, the error functions vary significantly in time intervals less than 1 msec. These functions approach $-\infty$ at t = 0, according to (66), except for $\phi = -\pi/2$.

The corresponding complex envelope is given by (72); its magnitude is plotted in figure 4 over a much wider time interval. The straight line just to the right of the origin is the desired exponential decay $a(t) = \exp(-\alpha t)$, which dominates the error e(t) in this region of time. Eventually, however, for larger t or negative t, the error e(t) dominates, with its much slower decay rate. It is readily verified that the asymptotic behavior predicted by (75) is in control and very accurate near both edges of figure 4.

At the transition between the two components, the random vector addition in (72) leads to large oscillations; the period of the carrier is $1/f_o = 10$ msec, meaning that the transition oscillations in figure 4 have been grossly undersampled with the time increment Δ_t approximately 40 msec that was used. The error curve for $\phi = 0$ is much smaller than the other two examples over

most of its range; however, the magnitude error goes sharply to ∞ at $t = 0$.

From (72) and figure 4, it is seen that for $\phi = -\pi/2$, the phase $P(t)$ of complex envelope $\underline{y}(t)$ is essentially $-\pi/2$ for $t > 0$, until we reach the transition. To the right of the transition, the phase of $\underline{y}(t) \exp(i\omega_o t)$ is essentially $\pi/2$ because $e(t) > 0$ for $t > 0$, for this example. For $t < 0$, the phase of $\underline{y}(t) \exp(i\omega_o t)$ is $-\pi/2$ because $e(t) < 0$ for $t < 0$. We will numerically confirm these claims later when we compute the analytic waveform and complex envelope by means of FFTs.

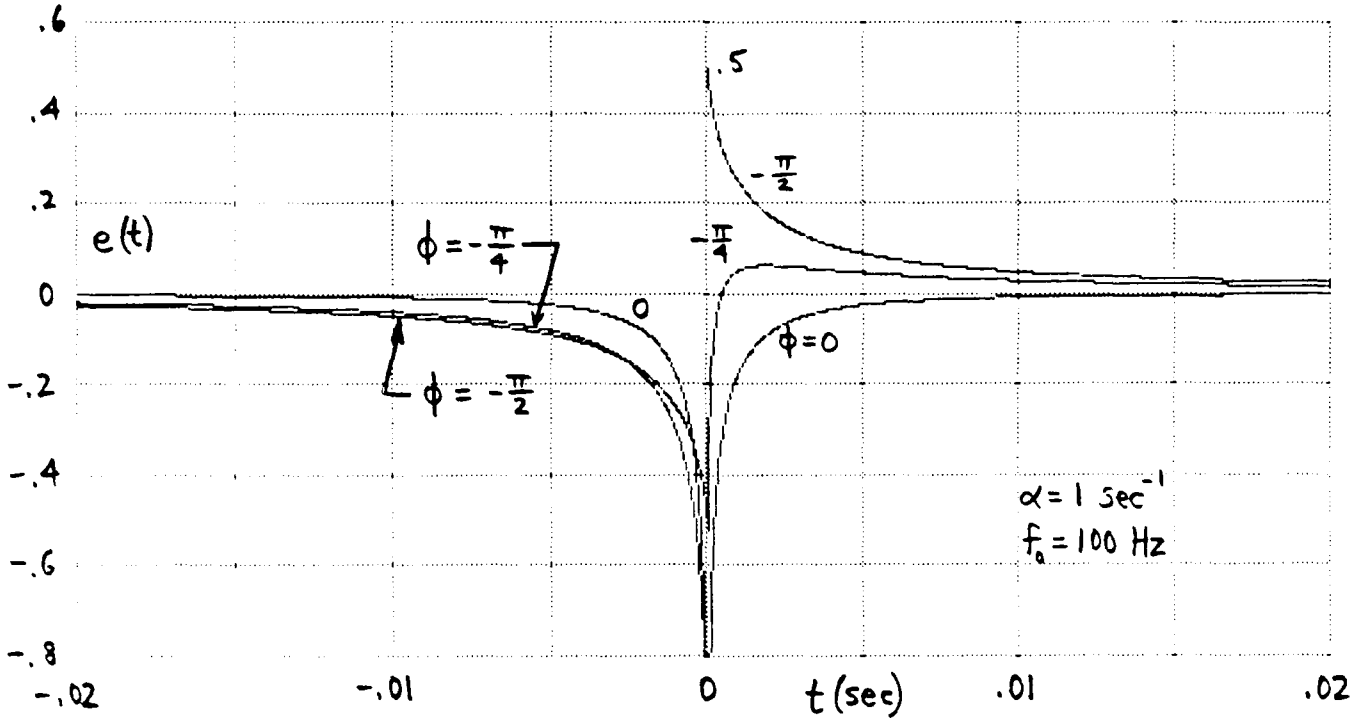

Figure 3. Error e(t) for Various ϕ

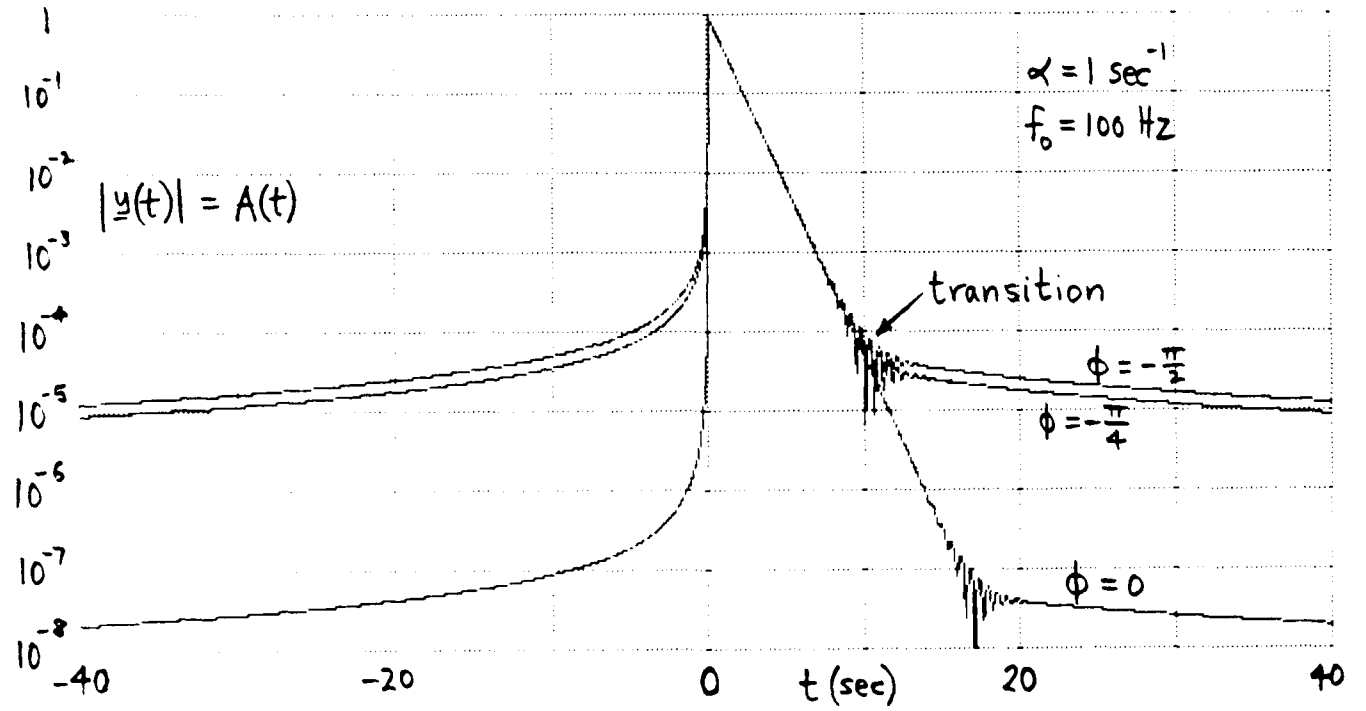

Figure 4. Complex Envelope for Various ϕ

FILTERED COMPLEX ENVELOPE

It was shown in (26) that the spectrum $\underline{Y}(f)$ of the complex envelope $\underline{y}(t)$ of a given waveform $y(t)$ with complex imposed modulation $z(t)$ is given by a desired term $Z(f)$ plus an undesired error term, namely,

$$\underline{Y}(f) = Z(f) + i\, E(f+f_o) \ . \tag{82}$$

According to figures 1 and 2, the major contribution of the first term, $Z(f)$, is centered around $f = 0$, while the undesired second term in (82) is centered about $f = -f_o$. This suggests the possibility of lowpass filtering complex envelope spectrum $\underline{Y}(f)$ in order to suppress the undesired frequency components. Also, this will eliminate or suppress the undesired logarithmic singularities present in the complex envelope $\underline{y}(t)$.

LOWPASS FILTER

To this aim, let $H(f)$ denote a lowpass filter with $H(0) = 1$ and cutoff frequency, f_1, smaller than f_o. For example, the Hann filter is characterized by

$$H(f) = \left\{ \begin{array}{ll} \cos^2\left(\frac{\pi}{2}\,\frac{f}{f_1}\right) & \text{for } |f| < f_1 \\ \\ 0 & \text{otherwise} \end{array} \right\} \ . \tag{83}$$

The filtered complex envelope spectrum is, in general,

$$G(f) = \underline{Y}(f)\ H(f) \ . \tag{84}$$

The importance of having $f_1 < f_o$ is that filter H(f) will then smoothly cut off its response before reaching the discontinuity at $f = -f_o$ of the spectrum $\underline{Y}(f)$ of the complex envelope $\underline{y}(t)$; see (27). In this way, we can avoid the slowly decaying behavior of the complex envelope $\underline{y}(t)$ for large t, namely 1/t, which inherently accompanies its discontinuous frequency spectrum. This will prove important when we numerically evaluate the filtered complex envelope, by sampling (84) at equispaced frequencies and performing a Fourier transform into the t domain, necessarily encountering the unavoidable aliasing in time associated with such a technique.

Since the complex envelope $\underline{y}(t)$ is given by (25) as the sum of desired component z(t) and an error term, the filtered waveform corresponding to spectrum G(f) in (84) is given by

$$g(t) = \underline{y}(t) \oplus h(t) =$$

$$= z(t) \oplus h(t) + [i\, e(t) \exp(-i2\pi f_o t)] \oplus h(t) = \qquad (85)$$

$$= g_d(t) + g_u(t) \ , \qquad (86)$$

where $\oplus$ denotes convolution, h(t) is the impulse response of the general filter H(f) in (84), and $g_d(t)$ and $g_u(t)$ are, respectively, the desired and undesired components of the filtered complex envelope g(t). We should choose filter H(f) to be real and even; then impulse response h(t) is also real and even.

The Hann filter example in (83) could be replaced by a filter with a flatter response about f = 0 and a sharper cutoff

behavior. The major features that filter H(f) should have are a fairly flat response in the Z(f) frequency range near f = 0, but cut off significantly before getting into the major frequency content of error term $E(f+f_o)$, which is centered about $f = -f_o$. If the given waveform y(t) in (1) is not really narrowband, there may not be any good choice of cutoff frequency f_1; that is, it may be necessary to sacrifice some of the higher frequency content of z(t) or to allow some of the error e(t) to pass.

EXAMPLE

We again consider the example given in (47) and (48), along with the Hann filter in (83). In order to evaluate the filtered complex envelope g(t) in (86), we define an auxiliary function

$$E(z) = \exp(z)\, E_1(z) \ , \tag{87}$$

where $E_1(z)$ is the exponential integral [3; 5.1.1]. Then, when we use the fact that (83) can be expressed as

$$H(f) = \frac{1}{2} + \frac{1}{4}\exp(i\pi f/f_1) + \frac{1}{4}\exp(-i\pi f/f_1) \quad \text{for } |f| < f_1 \ , \tag{88}$$

we encounter the following two integrals. First, we need the result

$$\int_{-f_1}^{f_1} df\ \frac{\exp(i\omega t + i\omega\frac{1}{2}n/f_1)}{\alpha + i2\omega_o + i\omega} = \frac{(-1)^n}{i2\pi}\left[\exp(-i\omega_1 t)E(u_n) - \exp(i\omega_1 t)E(v_n)\right] \ , \tag{89}$$

where $\omega = 2\pi f$, n is an integer, $f_1 < f_o$, and we defined

$$u_n = -(\alpha + i2\omega_o - i\omega_1)(t + \tfrac{1}{2}n/f_1) ,$$
$$v_n = -(\alpha + i2\omega_o + i\omega_1)(t + \tfrac{1}{2}n/f_1) . \qquad (90)$$

To derive this result, we let $x = -(\alpha + i2\omega_o + i\omega)(t + \frac{1}{2}n/f_1)$ in (89) and used [3; 5.1.1], along with the important fact that $f_1 < f_o$, which guarantees no crossing of the negative real axis of the resulting contour of integration in the complex x-plane.

Also, when we define

$$\underline{u}_n \equiv u_n(f_o=0) = -(\alpha - i\omega_1)(t + \tfrac{1}{2}n/f_1) ,$$
$$\underline{v}_n \equiv v_n(f_o=0) = -(\alpha + i\omega_1)(t + \tfrac{1}{2}n/f_1) , \qquad (91)$$

then for $f_o = 0$, we find the second integral result required, namely,

$$\int_{-f_1}^{f_1} df \, \frac{\exp(i\omega t + i\omega\tfrac{1}{2}n/f_1)}{\alpha + i\omega} = \frac{(-1)^n}{i2\pi}\left[\exp(-i\omega_1 t)E(\underline{u}_n) - \exp(i\omega_1 t)E(\underline{v}_n)\right] +$$
$$+ U(t + \tfrac{1}{2}n/f_1)\, \exp(-\alpha t - \tfrac{1}{2}\alpha n/f_1) . \qquad (92)$$

The extra term in the second line of (92) is due to a crossing of the negative real axis in the complex x-plane by the contour of integration when we make the substitution $x = -(\alpha + i\omega)(t + \frac{1}{2}n/f_1)$ in the integral of (92).

The desired component of the filtered complex envelope is given by the first term of (85) and (86), in the alternative form

$$g_d(t) = \int df\ \exp(i2\pi ft)\ Z(f)\ H(f) =$$

$$= \int_{-f_1}^{f_1} df\ \exp(i2\pi ft)\ \frac{\exp(i\phi)}{\alpha + i\omega}\ \cos^2\left(\frac{\pi}{2}\ \frac{f}{f_1}\right) = \tag{93}$$

$$= e^{i\phi}\left(e^{-\alpha t}\left[\frac{1}{2}U(t) + \frac{1}{4}U\left(t + \frac{1}{2f_1}\right)\ \exp\left(\frac{-\alpha}{2f_1}\right) + \frac{1}{4}U\left(t - \frac{1}{2f_1}\right)\ \exp\left(\frac{\alpha}{2f_1}\right)\right] +\right.$$

$$+ \frac{1}{i4\pi}\left(\exp(-i\omega_1 t)\left[E(\underline{u}_0) - \frac{1}{2}\ E(\underline{u}_1) - \frac{1}{2}\ E(\underline{u}_{-1})\right] -\right.$$

$$\left.\left. - \exp(i\omega_1 t)\left[E(\underline{v}_0) - \frac{1}{2}\ E(\underline{v}_1) - \frac{1}{2}\ E(\underline{v}_{-1})\right]\right)\right) . \tag{94}$$

Here, we also used (48), (88), and (92). Since the factor multiplying $\exp(i\phi)$ in (93) has conjugate symmetry in frequency f, the time function multiplying $\exp(i\phi)$ in (94) is purely real for all time t.

The undesired spectral component in (82) is given by

$$i\ E(f+f_o) = Z^*(-f-2f_o) \quad \text{for } f > -f_o\ , \tag{95}$$

where we used (22). Therefore, using restriction $f_1 < f_o$, the undesired time component in the filtered complex envelope in (86) is given, upon use of (89), by

$$g_u(t) = \int_{-f_1}^{f_1} df\ \exp(i2\pi ft)\ \frac{\exp(-i\phi)}{\alpha + i2\omega_o + i\omega}\ \cos^2\left(\frac{\pi}{2}\ \frac{f}{f_1}\right) =$$

$$= \frac{\exp(-i\phi)}{i4\pi}\left(\exp(-i\omega_1 t)\left[E(u_0) - \frac{1}{2}\ E(u_1) - \frac{1}{2}\ E(u_{-1})\right] -\right.$$

$$\left. - \exp(i\omega_1 t)\left[E(v_0) - \frac{1}{2}\ E(v_1) - \frac{1}{2}\ E(v_{-1})\right]\right) . \tag{96}$$

In contrast with (94), the time function multiplying phase factor $\exp(-i\phi)$ in (96) is complex. The total time waveform at the filter output, $g(t)$, namely the filtered complex envelope, is given by (94) plus (96), and depends on ϕ. In fact, since the magnitude of total output $g(t)$ depends on ϕ, we will look at plots of the magnitudes of components $|g_d(t)|$ and $|g_u(t)|$, neither of which depend on ϕ.

For comparison, the complex envelope itself is given by (25) in the form $\underline{y}(t) = z(t) + i\, e(t) \exp(-i2\pi f_o t)$. Since these two (unfiltered) components depend differently on phase ϕ, we shall also consider only their magnitudes $|z(t)|$ and $|e(t)|$ and compare them with filtered components $|g_d(t)|$ and $|g_u(t)|$, respectively. In particular, from (48), the desired component of the complex envelope $\underline{y}(t)$ for the example at hand is

$$z(t) = \exp(i\phi - \alpha t)\, U(t) \quad \text{for all } t\ , \tag{97}$$

while the undesired portion is given by (56) and (87) as

$$e(t) = -\frac{1}{\pi}\mathrm{Re}\{\exp(i\phi - ct)\, E_1(-ct)\} = -\frac{1}{\pi}\mathrm{Re}\{\exp(i\phi)\, E(-ct)\} \tag{98}$$

for $t \neq 0$, where $c = \alpha - i\omega_o$. The magnitude of complex waveform $z(t)$ is independent of ϕ, but the magnitude of real error waveform $e(t)$ still depends on ϕ; see figure 3.

The magnitudes of $z(t)$ and $g_d(t)$ for $\alpha = 1\ \mathrm{sec}^{-1}$ and $f_1 = 40$ Hz are displayed in figure 5 on a logarithmic ordinate. The filtered complex envelope component, $g_d(t)$, drops very quickly to the left of $t = 0$ and is indistinguishable from $z(t)$ for $t > 0$; compare with figure 4. Thus, the passband of the Hann

filter H(f) in (83) has been taken wide enough to pass the majority of the frequency components of desired function Z(f) in this example. The darkened portion of the plot just to the left of t = 0 corresponds to a weak amplitude-modulated 40 Hz component, which is the cutoff frequency f_1 of filter H(f).

The magnitudes of $g_u(t)$ and error e(t) are displayed in figure 6 for the additional choice of parameters f_o = 100 Hz and $\phi = -\pi/2$ rad. The peak values of these undesired components at t = 0 differ by over a factor of 10, through this process of filtering the complex envelope. At the same time, the skirts of filtered version $g_u(t)$ are down by several orders of magnitude relative to e(t). The thick plot of $|g_u(t)|$ is again a 40 Hz component, which has been sampled at a time increment Δ_t = .002 sec.

For phase ϕ = 0 instead, original waveform y(t) in (45) is discontinuous at t = 0, giving rise to a Hilbert transform which has a logarithmic infinity there; see (77), (78), and (79). Therefore, the magnitude of error e(t) in figure 7 has an infinity at t = 0, whereas the filtered quantity $g_u(t)$ is finite there; in fact, $|g_u(t)|$ is independent of ϕ. Although e(t) is significantly reduced in value, away from the origin, relative to figure 6, it is still larger than the filtered quantity $g_u(t)$. Since the energy in error waveform e(t) is independent of ϕ (see (62)), smaller skirts in e(t) can only be accompanied by a larger peak; in fact, this latter case for e(t) in figure 7 has an infinite (integrable) peak at t = 0. By contrast, the energy in the filtered undesired component $g_u(t)$ is, from (82) and (84),

$$\int df \, |E(f+f_o)|^2 \, |H(f)|^2 \, , \qquad (99)$$

which can be considerably less than the error energy, when filter H(f) significantly rejects the displaced error spectrum $E(f+f_o)$.

This example points out that considerable reduction of the undesired error term in the complex envelope can be achieved through the use of lowpass filtering with an appropriate cutoff frequency, and that the undesired singularities can be significantly suppressed. Furthermore, the desired component of the complex envelope can be essentially retained. These conclusions follow if the bandwidth of the imposed modulation, z(t) in (1) and (2), is small relative to the carrier frequency f_o.

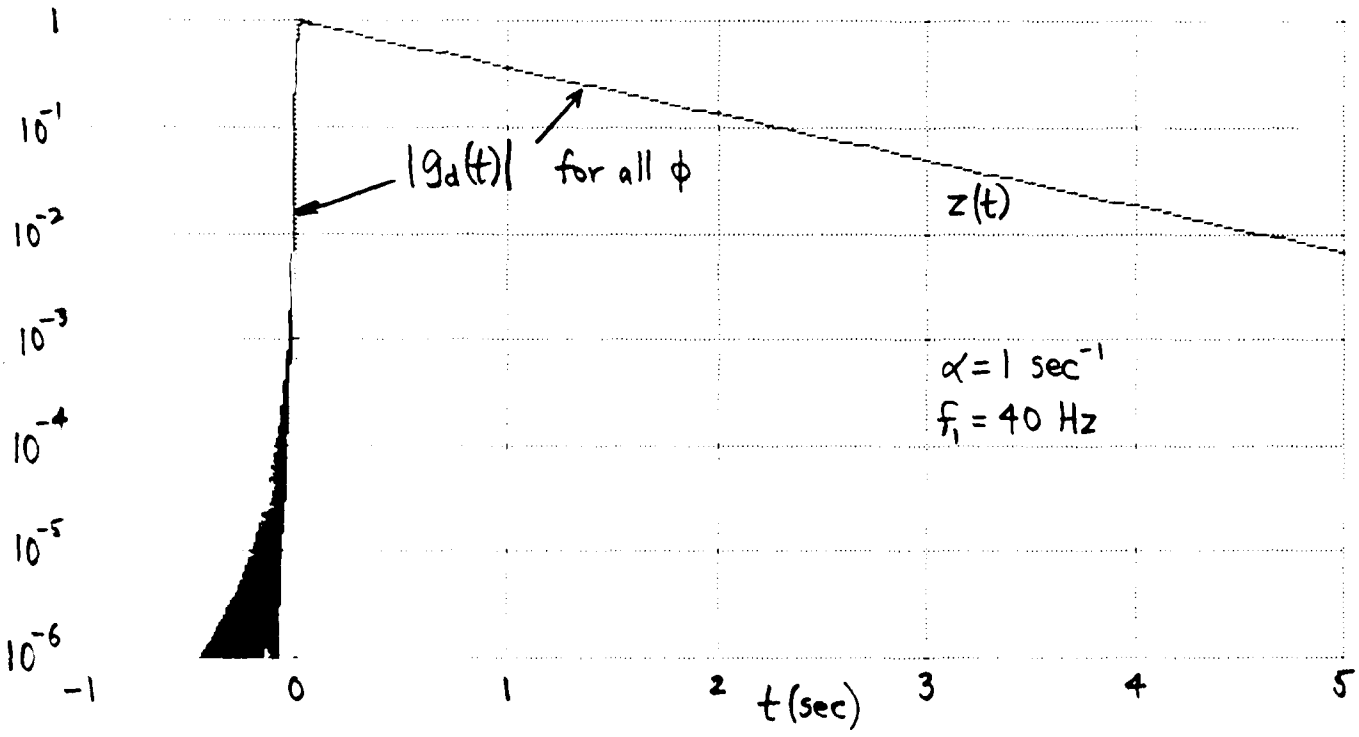

Figure 5. Filtered Complex Envelope; Desired Terms

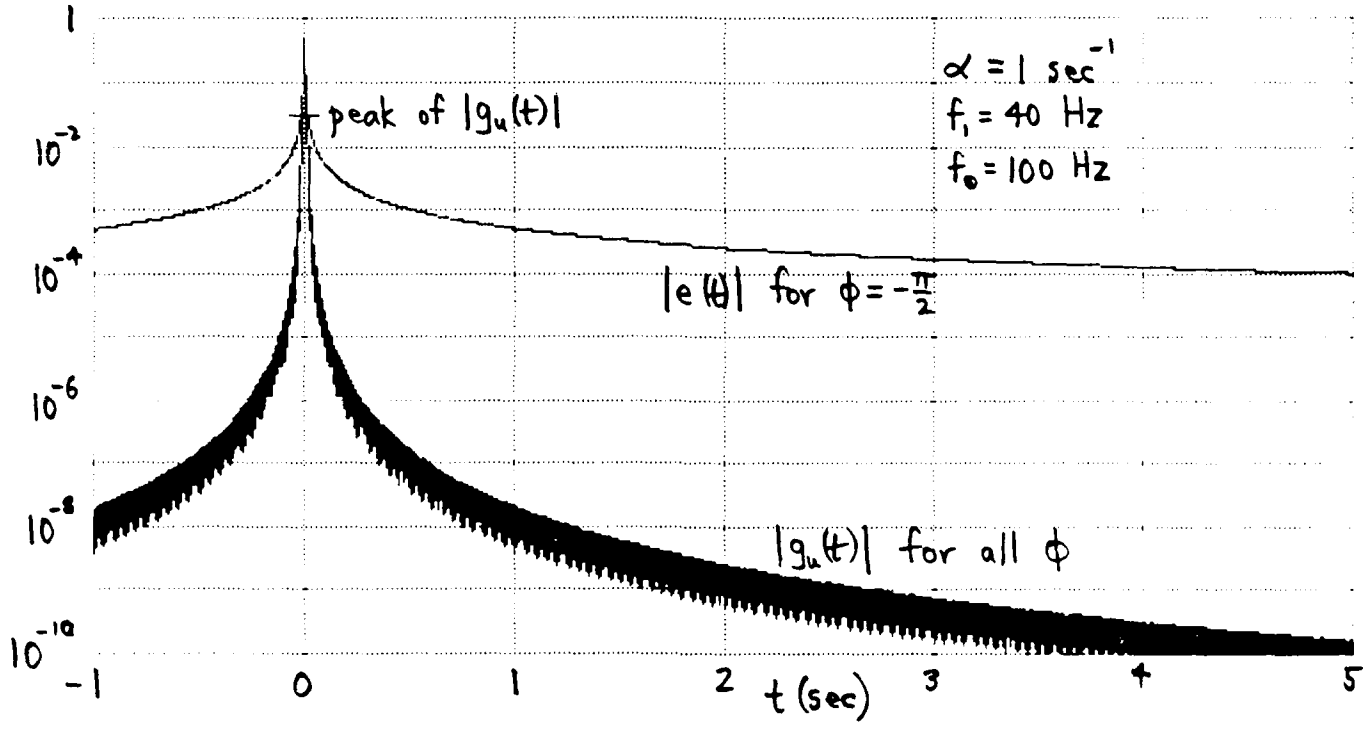

Figure 6. Filtered Complex Envelope; Undesired Terms, $\phi=-\pi/2$

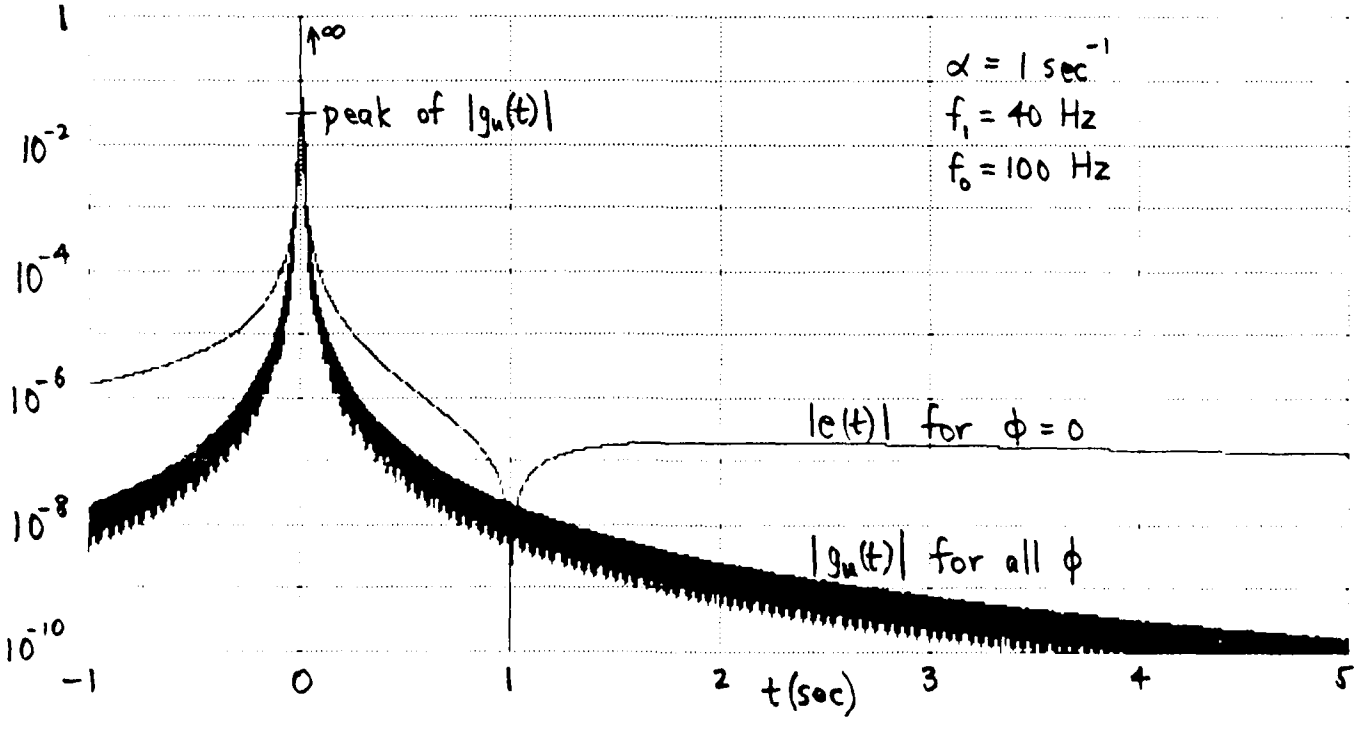

Figure 7. Filtered Complex Envelope; Undesired Terms, $\phi=0$

TRAPEZOIDAL APPROXIMATIONS TO ANALYTIC WAVEFORM, COMPLEX ENVELOPE, AND FILTERED COMPLEX ENVELOPE

In this section, we address methods of evaluating the analytic waveform and the complex envelope by means of FFTs. We start by repeating the results in (6) and (8) for the analytic waveform, that is,

$$Y_+(f) = 2\ U(f)\ Y(f)\ , \tag{100}$$

$$y_+(t) = \int df\ \exp(i2\pi ft)\ Y_+(f) = \int_0^\infty df\ \exp(i2\pi ft)\ 2\ Y(f)\ . \tag{101}$$

The trapezoidal approximation to (101) is obtained by sampling with frequency increment Δ to get

$$\tilde{y}_+(t) \equiv \Delta \sum_{n=0}^{\infty} \varepsilon_n\ \exp(i2\pi n\Delta t)\ 2\ Y(n\Delta) = \tag{102}$$

$$= \int_0^\infty df\ \exp(i2\pi ft)\ 2\ Y(f)\ \Delta\ \delta_\Delta(f) =$$

$$= y_+(t) \oplus \delta_{1/\Delta}(t) = \sum_n y_+\left(t - \frac{n}{\Delta}\right)\ , \tag{103}$$

where sequence $\varepsilon_0 = \frac{1}{2}$ and $\varepsilon_n = 1$ for $n \geq 1$, and summations without limits are from $-\infty$ to $+\infty$.

Notice that approximation $\tilde{y}_+(t)$ is a continuous function of time t and has period $1/\Delta$ in t. The desired term in (103) is that for n = 0, namely analytic waveform $y_+(t)$. Because $y_+(t)$ can contain a slowly decaying Hilbert transform component, the aliasing at separation $1/\Delta$ in (103) can lead to severe distortion

in approximation $\tilde{y}_+(t)$ defined in (102).

Since $\tilde{y}_+(t)$ has period $1/\Delta$ in t, we can confine its computation to any interval of length $1/\Delta$. In particular, if we divide this interval into N equally-spaced points (where integer N is arbitrary), we can compute, from (102),

$$\tilde{y}_+\left(\frac{k}{N\Delta}\right) = \Delta \sum_{n=0}^{\infty} \varepsilon_n \exp(i2\pi nk/N)\ 2\ Y(n\Delta) \qquad (104)$$

for any N contiguous values of k. If we choose the range $0 \le k \le N-1$, and if we collapse the infinite sequence in the summand of (104) according to

$$z_n = 2\Delta \sum_{j=0}^{\infty} \varepsilon_{n+jN}\ Y(n\Delta + jN\Delta) \quad \text{for } 0 \le n \le N-1\ , \qquad (105)$$

then (104) can be written precisely as

$$\tilde{y}_+\left(\frac{k}{N\Delta}\right) = \sum_{n=0}^{N-1} \exp(i2\pi nk/N)\ z_n\ . \qquad (106)$$

This last result can be accomplished by means of an N-point FFT if N is highly composite. This is a very efficient method of computing the aliased version of the analytic waveform as defined by (102).

COMPLEX ENVELOPE

The center frequency f_c of single-sided spectrum $Y_+(f)$ in (100) can be found by the method described in appendix A. Then the complex envelope spectrum and waveform are, respectively,

$$\underline{Y}(f) = Y_+(f+f_c) \ , \tag{107}$$

$$\underline{y}(t) = \int df \ \exp(i2\pi ft) \ \underline{Y}(f) =$$

$$= \int df \ \exp(i2\pi ft) \ Y_+(f+f_c) = \exp(-i2\pi f_c t) \ y_+(t) \ . \tag{108}$$

The approximation to complex envelope $\underline{y}(t)$ is achieved by relating it to that for analytic waveform $y_+(t)$ according to

$$\tilde{\underline{y}}(t) \equiv \exp(-i2\pi f_c t) \ \tilde{y}_+(t) = \tag{109}$$

$$= \exp(-i2\pi f_c t) \ \Delta \sum_{n=0}^{\infty} \varepsilon_n \ \exp(i2\pi n\Delta t) \ 2 \ Y(n\Delta) \ , \tag{110}$$

where we used (108) and (102). The continuous function $\exp(i2\pi f_c t) \ \tilde{\underline{y}}(t)$, which is just $\tilde{y}_+(t)$, has period $1/\Delta$ in t, which simplifies its calculation. Using (109), (103), and (108), there follows, for the approximation to the complex envelope,

$$\tilde{\underline{y}}(t) = \exp(-i2\pi f_c t) \sum_n y_+\left(t - \frac{n}{\Delta}\right) = \sum_n \underline{y}\left(t - \frac{n}{\Delta}\right) \exp(-i2\pi f_c n/\Delta) \ . \tag{111}$$

The desired term in (111), for n = 0, is complex envelope $\underline{y}(t)$. The n-th term has a time delay (aliasing) of n/Δ and a phase shift of $n2\pi f_c/\Delta$ radians, which is arbitrary because frequency

sampling increment Δ in (102) is unrelated to center frequency f_c of $Y_+(f)$ in (100).

Sample values of complex envelope approximation $\tilde{\underline{y}}(t)$ can be obtained from (110) as

$$\tilde{\underline{Y}}\left(\frac{k}{N\Delta}\right) = \exp\left(-i2\pi f_c \frac{k}{N\Delta}\right) \Delta \sum_{n=0}^{\infty} \varepsilon_n \exp(i2\pi nk/N)\ 2\ Y(n\Delta) \ . \quad (112)$$

Again, the infinite sum in (112) can be collapsed and realized as an N-point FFT; see (104) - (106). The phase factor $p_k = \exp(-i2\pi f_c k/(N\Delta))$ can be computed via recurrence $p_k = p_{k-1} \exp(-i2\pi f_c/(N\Delta))$.

FILTERED COMPLEX ENVELOPE

The spectrum of the filtered complex envelope is given by (84) as $G(f) = \underline{Y}(f)\ H(f)$. The filtered complex envelope waveform is

$$g(t) = \int df \exp(i2\pi ft)\ G(f) = \underline{y}(t) \oplus h(t) \quad (113)$$

and has low sidelobes and rapid decay in t, when filter H(f) is chosen appropriately.

The approximation to g(t) adopted here will be generalized slightly in order to allow for frequency-shifted sampling. Specifically, we define

$$\tilde{g}_\alpha(t) \equiv \int df\ \exp(i2\pi ft)\ G(f)\ \Delta\ \delta_\Delta(f - \alpha) = \tag{114}$$

$$= \Delta \sum_n \exp(i2\pi[n\Delta + \alpha]t)\ G(n\Delta + \alpha)\ . \tag{115}$$

The function $\exp(-i2\pi\alpha t)\ \tilde{g}_\alpha(t)$ has period $1/\Delta$ in t, which allows us to confine its calculation to any convenient period.

The behavior of approximation $\tilde{g}_\alpha(t)$ in (114) follows as

$$\tilde{g}_\alpha(t) = g(t) \oplus [\exp(i2\pi\alpha t)\ \delta_{1/\Delta}(t)] =$$

$$= g(t) \oplus \sum_n \exp(i2\pi\alpha n/\Delta)\ \delta\left(t - \frac{n}{\Delta}\right) =$$

$$= \sum_n \exp(i2\pi\alpha n/\Delta)\ g\left(t - \frac{n}{\Delta}\right)\ . \tag{116}$$

This is the aliased version of the filtered complex envelope. The desired term, for n = 0, is the filtered complex envelope g(t), independent of the choice of frequency shift α. Shift α is arbitrary and could be taken as $-f_c$ if desired.

Samples of $\tilde{g}_\alpha(t)$ are available from (115) according to

$$\tilde{g}_\alpha\left(\frac{k}{N\Delta}\right) = \Delta\ \exp\left(i2\pi\alpha\ \frac{k}{N\Delta}\right) \sum_n \exp(i2\pi nk/N)\ G(n\Delta + \alpha)\ , \tag{117}$$

which we can limit to $0 \le k \le N-1$ due to the periodicity of $\tilde{g}_\alpha(t)$. Again, the infinite sum on n can be converted to an N-point FFT without error, by collapsing into the finite sequence

$$z_n = \Delta \sum_j G(n\Delta + \alpha + jN\Delta) \quad \text{for } 0 \le n \le N-1\ . \tag{118}$$

The remaining phasor $\exp(i2\pi\alpha k/(N\Delta))$ in (117) can be quickly obtained via recursion on k.

GRAPHICAL RESULTS

The same fundamental example introduced in (45) will be used here, again with $\alpha = 1$ sec^{-1} and $f_o = 100$ Hz. For phase $\phi = -\pi/2$, FFT size $N = 1024$, and a frequency increment of $\Delta = 1/80$ Hz, the magnitude of $\tilde{y}(t)$, namely $\tilde{A}(t)$, is displayed in figure 8 over the $1/\Delta = 80$ sec period centered at $t = 0$. This selection of the time period has been purposely made the same as that used in figure 4, for easy comparison of results. The major difference between the $\phi = -\pi/2$ result in figure 4 and figure 8 is that the aliasing in the latter case causes the curve to have a jagged behavior and to droop in the neighborhood of $t = \pm 40$ sec. However, other examples could well have the aliasing increase near the edges of the period. A total of 88,000 samples of Y(f) at frequency increment Δ were taken in computation of (104); the collapsing in (106) resulted in storage of only $N = 1024$ complex numbers and the ability to use a single relatively small N-point FFT. A program for the evaluation of the complex envelope by means of an FFT with collapsing is furnished in appendix B; the FFT uses a zero-subscripted array in direct agreement with the mathematical definition of the FFT.

The corresponding phase, $\tilde{P}(t) = \arg\{\tilde{y}(t)\}$, of the aliased complex envelope is given in figure 9. The phase is approximately $-\pi/2$ for $0 \leq t \leq 10$ sec, as expected, since in

this limited time interval, the error is not the dominant term. However, over the rest of the period, the error term does dominate and it has an $\exp(-i\omega_o t)$ behavior, where $f_o = 100$; see (25) and figure 3. Thus, the time sampling increment $\Delta_t = 1/(N\Delta) = .078$ sec is grossly inadequate to track this high-frequency term, and we get virtually random samples of the phase of the complex exponential $\exp(-i\omega_o t)$.

To confirm the phase behavior outside the (0,10) sec interval, we have plotted the phase of $\underline{y}(t)\exp(i\omega_o t) = y_+(t)$ in figure 10 as found by the FFT procedure above. To the right of $t = 10$, the phase is approximately $\pi/2$, in agreement with the fact that $e(t)$ is real and positive for $t > 0$; see figure 3 and (25). For time $t < 0$, the phase is $-\pi/2$ because $e(t) < 0$ for $t < 0$. The oscillatory behavior at both edges of the period, namely, for $30 < |t| < 40$, is due to aliasing from adjacent lobes indicated by (103) and (111).

When ϕ is changed to 0 and everything else is kept unchanged, the result for the magnitude of complex envelope aliased version $\tilde{\underline{y}}(t)$ is plotted in figure 11. Comparison with the exact results in figure 4 reveals a very dramatic increase in aliasing, in fact, by <u>two</u> orders of magnitude. The reason for this considerable increase can be seen from figure 3 and (75); namely, the error $e(t)$ is unipolar for $\phi = 0$ and it decays very slowly. Whereas for figure 8, the alternating character of the overlapping aliased error lobes led to a cancellation near $t = \pm 40$ sec, the opposite situation occurred in figure 11, leading to a

considerable build-up of the aliasing effect.

The corresponding phase of $\tilde{y}(t)$, $\tilde{P}(t)$, is plotted in figure 12. Its value is zero in the region $0 \leq t \leq 10$, as expected, since the desired term, $\exp(-\alpha t)$, dominates here. Outside this region, the situation is the same as explained above with respect to figure 9. We have not plotted the counterpart to figure 10 because no one error lobe dominates anywhere on the time scale; the result is a phase plot that looks random over the entire period of (-40,40) sec.

When the complex envelope spectrum is filtered according to the Hann filter in (83) - (86), the results for the sampled filtered complex envelope waveform, obtained by means of the collapsed FFT in (117) and (118) with $\alpha = 0$, are given in figures 13 and 14. There were 6400 frequency samples taken of G(f) with increment $\Delta = 1/80$ Hz and an FFT size of $N = 1024$ was utilized; see appendix B. A comparison of the magnitudes in figures 13 and 5 reveals virtually identical results; namely, the error and its inherent accompanying aliasing, that was present in figure 8, is absent from figure 13.

The corresponding phase plot of the FFT output is displayed in figure 14. In the region $0 \leq t \leq 24$ sec, where the desired $\exp(-\alpha t)$ term dominates, the FFT output phase is equal to the value of $\phi = -\pi/2$ for this example. When this example was rerun for $\phi = 0$, similar high quality results were obtained, except that the FFT output phase was zero. The benefits of filtering the complex envelope spectrum are well illustrated by the results of figures 13 and 14.

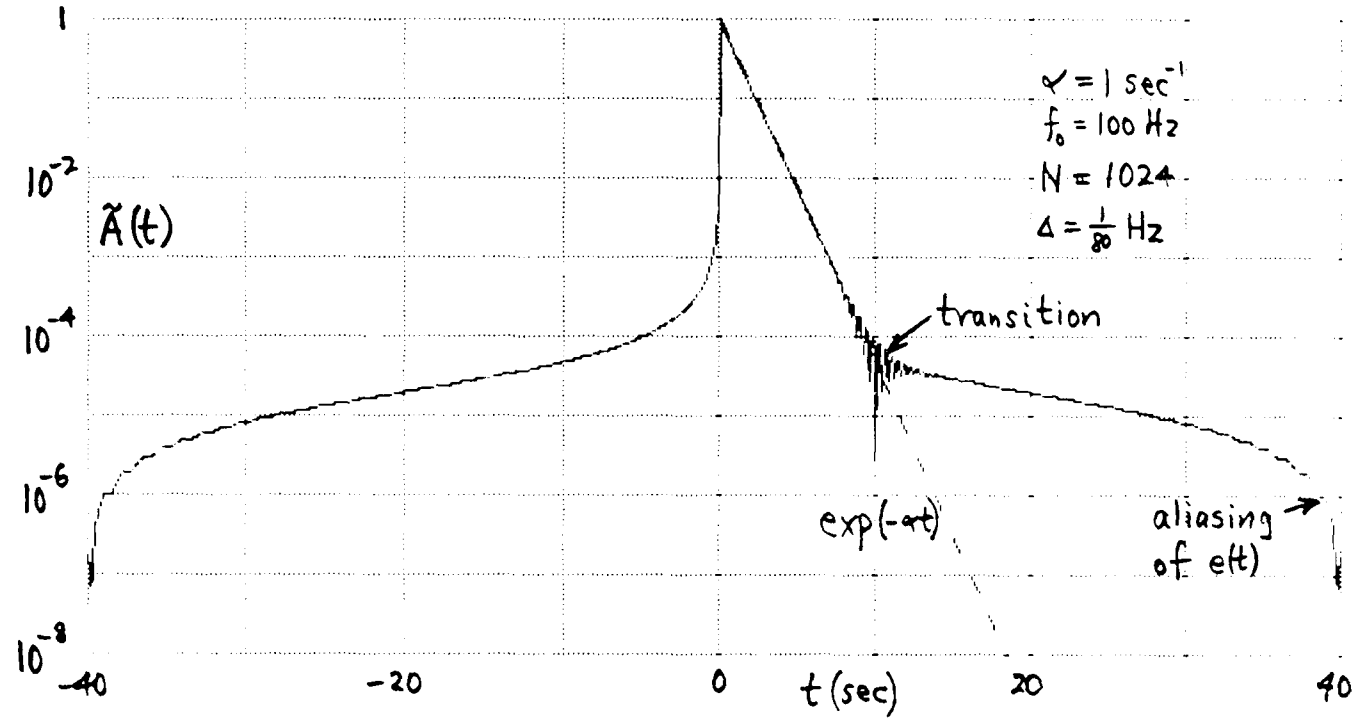

Figure 8. Magnitude of Complex Envelope via FFT, ϕ=-π/2

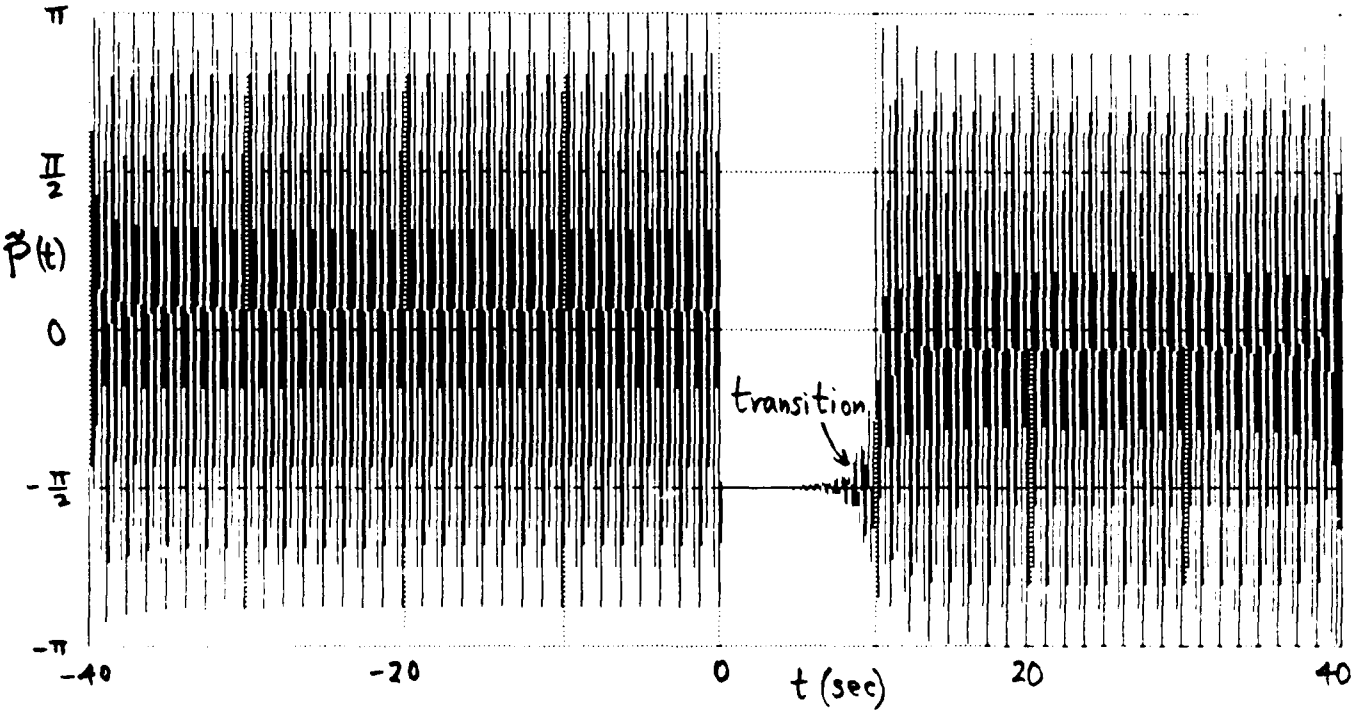

Figure 9. Phase of Complex Envelope via FFT, ϕ=-π/2

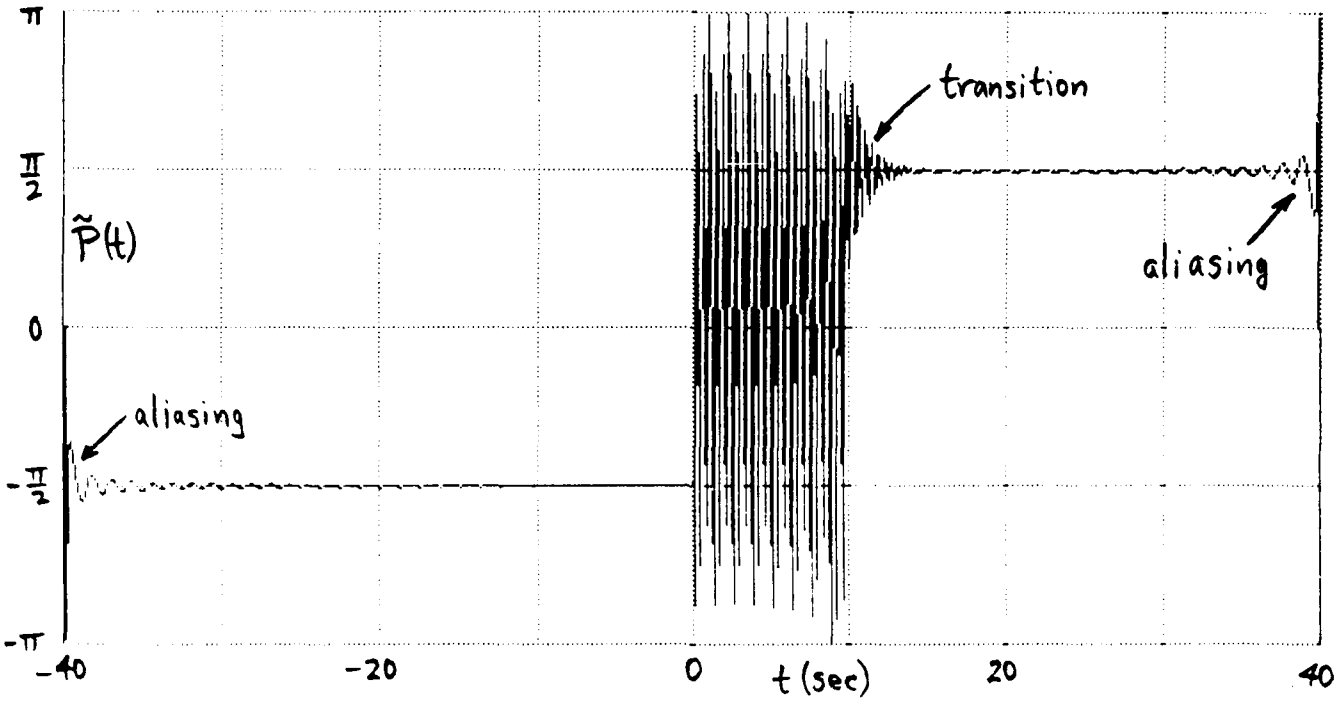

Figure 10. Phase of Analytic Waveform via FFT, $\phi=-\pi/2$

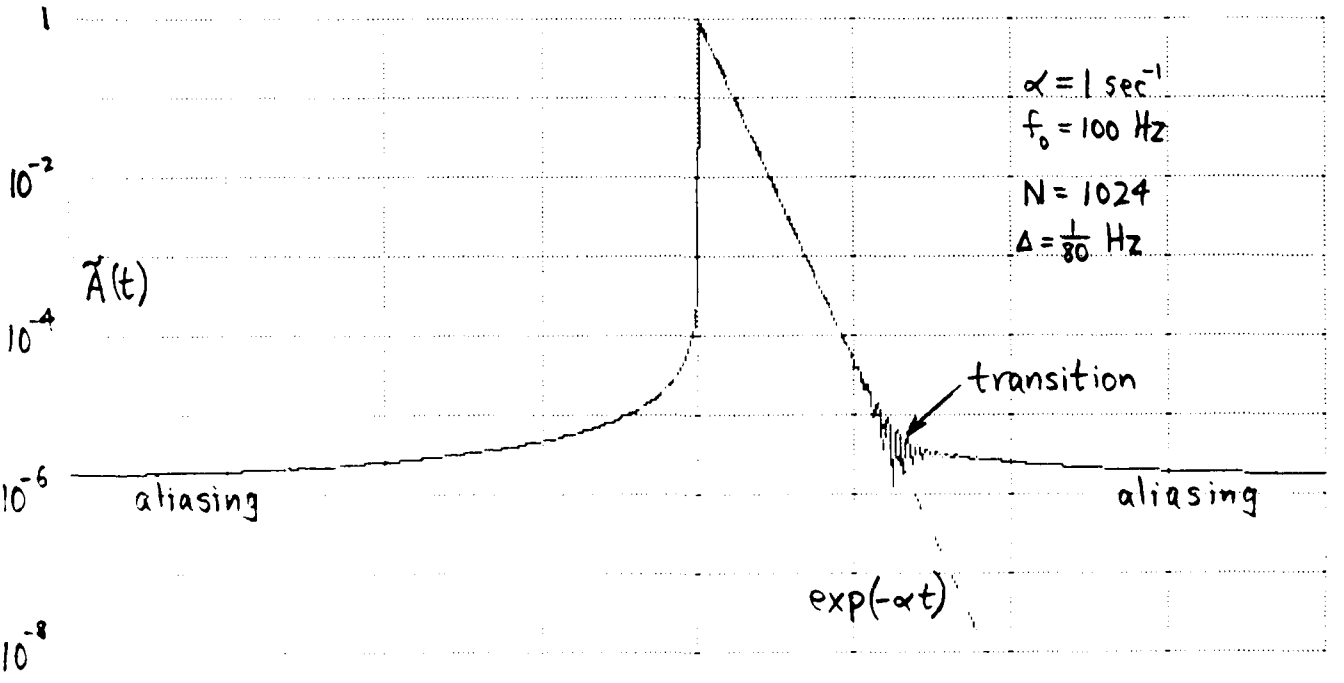

Figure 11. Magnitude of Complex Envelope via FFT, $\phi=0$

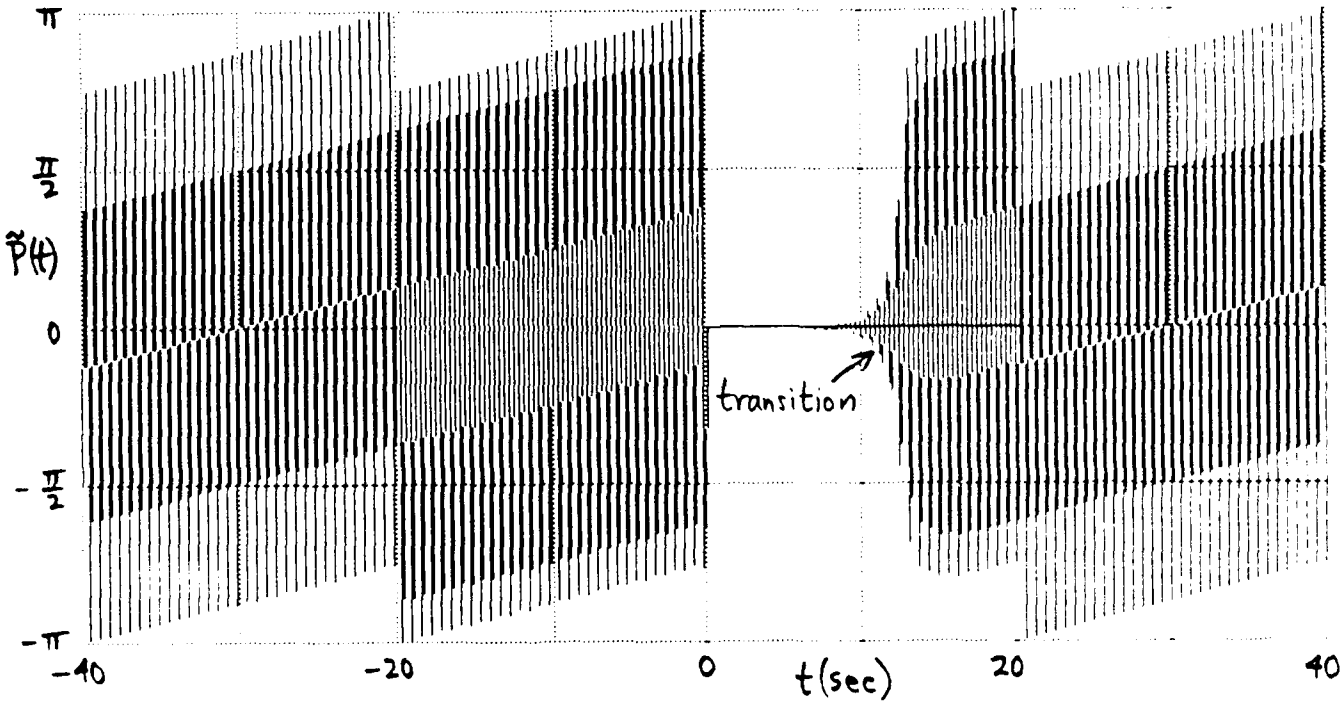

Figure 12. Phase of Complex Envelope via FFT, $\phi=0$

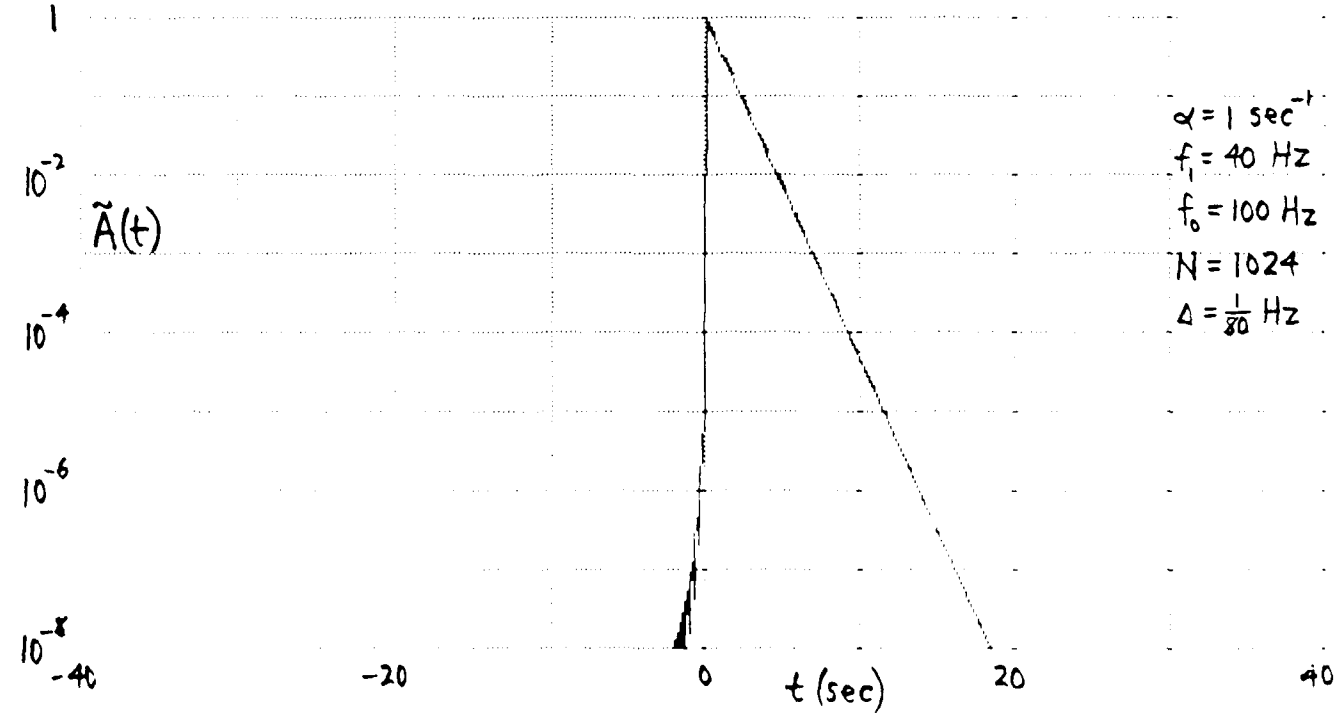

Figure 13. Magnitude of Filtered Complex Envelope via FFT, $\phi=-\pi/2$

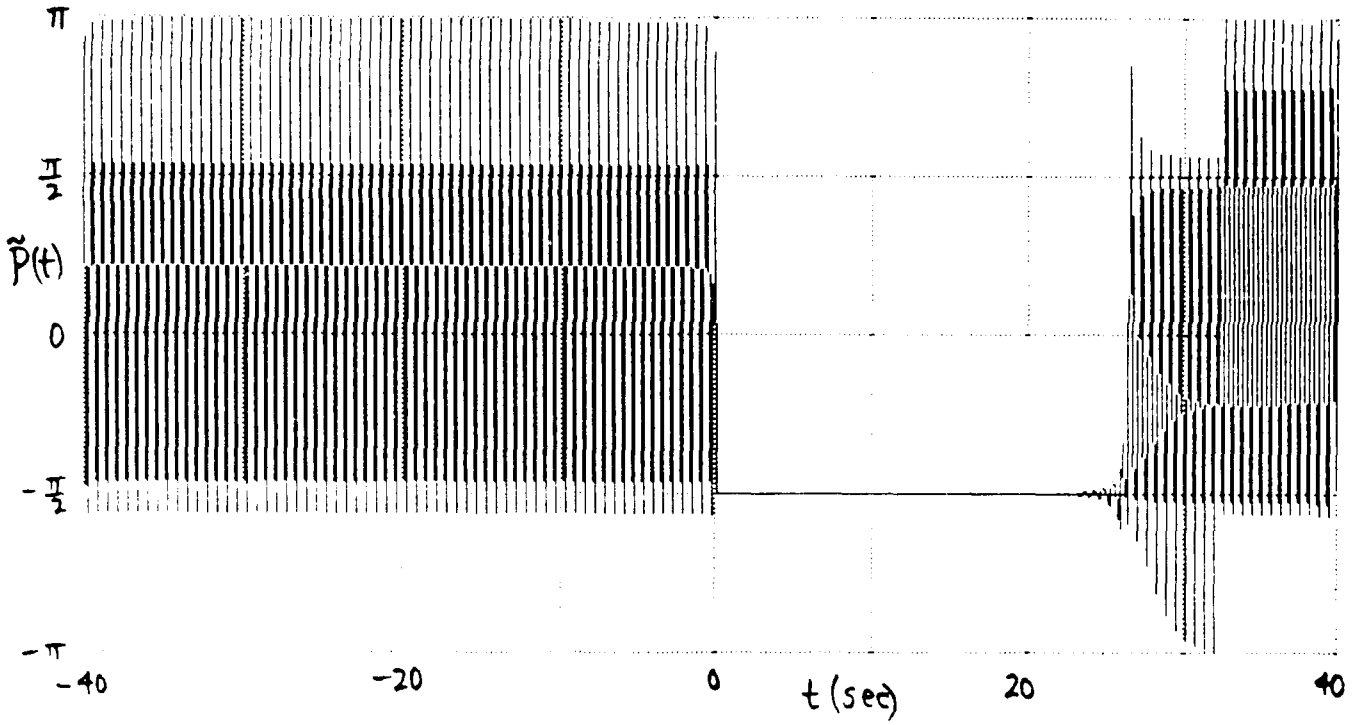

Figure 14. Phase of Filtered Complex Envelope via FFT, $\phi=-\pi/2$

ALIASING PROPERTIES OF COSINE AND SINE TRANSFORMS

If a time function is causal, it can be obtained from its Fourier transform either by a cosine or a sine transform. However, when these integral transforms are approximated, by means of sampling the frequency function and using some integration rule like trapezoidal, the "alias-free" interval in the time domain is approximately halved, as shown below. This does not necessarily mean that these transform alternatives should be discarded, because a more rapidly decaying integrand can be useful, but it does point out a cautionary feature in their use and the need to consider the tradeoff between aliasing and truncation error.

GENERAL TIME FUNCTION

In general, complex time function y(t) is obtained from its Fourier transform Y(f) according to

$$y(t) = \int df\ \exp(i2\pi ft)\ Y(f) = \tag{119}$$

$$= \int df\ \cos(2\pi ft)\ Y(f) + i \int df\ \sin(2\pi ft)\ Y(f) = \tag{120}$$

$$= y_e(t) + y_o(t) \quad \text{for all } t\ , \tag{121}$$

where complex functions $y_e(t)$ and $y_o(t)$ are the even and odd parts of function y(t), respectively.

CAUSAL COMPLEX TIME FUNCTION

Now suppose that y(t) is causal, but possibly complex; then

$$y(t) = 0 \quad \text{for } t < 0 \; . \tag{122}$$

Then, letting $t = -a$, $a > 0$, we have, from (122) and (121),

$$0 = y(-a) = y_e(-a) + y_o(-a) = y_e(a) - y_o(a) \quad \text{for } a > 0 \; . \tag{123}$$

That is,

$$y_o(a) = y_e(a) \quad \text{for } a > 0 \; . \tag{124}$$

Therefore, from (121) and (120), we have two alternatives for a causal complex time function y(t):

$$y(t) = 2 \int df \cos(2\pi ft)\, Y(f) \quad \text{for } t > 0 \; , \tag{125}$$

and

$$y(t) = i2 \int df \sin(2\pi ft)\, Y(f) \quad \text{for } t > 0 \; . \tag{126}$$

We need complex function Y(f) for negative as well as positive frequency arguments f, in order to determine causal complex function y(t), but we can utilize either a cosine or a sine transform.

NONCAUSAL REAL TIME FUNCTION

Now suppose instead that y(t) is real, but noncausal. Then, since spectrum $Y(-f) = Y^*(f)$, we can express (119) as

$$y(t) = 2\ \mathrm{Re} \int_0^\infty df\ \exp(i2\pi ft)\ Y(f) = \tag{127}$$

$$= 2\int_0^\infty df\ \cos(2\pi ft)\ Y_r(f) - 2\int_0^\infty df\ \sin(2\pi ft)\ Y_i(f) \quad \text{for all } t. \tag{128}$$

The first term in (128) is even part $y_e(t)$, while the second term in (128) is odd part $y_o(t)$; see (121). In this case of a real time function y(t), we need complex function Y(f) only for $f > 0$.

CAUSAL REAL TIME FUNCTION

Now let y(t) be both causal and real. Then using property $Y(-f) = Y^*(f)$ in (125) and (126), we obtain

$$y(t) = 4 \int_0^\infty df\ \cos(2\pi ft)\ Y_r(f) \quad \text{for } t > 0\ , \tag{129}$$

and

$$y(t) = -4 \int_0^\infty df\ \sin(2\pi ft)\ Y_i(f) \quad \text{for } t > 0\ . \tag{130}$$

Here, we need either $Y_r(f)$ or $Y_i(f)$, and then only for positive frequency arguments f. Also, a cosine or a sine transform will suffice for determination of y(t).

ALIASING PROPERTIES

The above relations have all assumed that spectrum Y(f) is available for all continuous f. Now we will address the effects of only having samples of Y(f) available at frequency increment Δ. We begin with the trapezoidal approximation to (119):

$$y_1(t) \equiv \Delta \sum_n \exp(i2\pi n\Delta t)\ Y(n\Delta) \quad \text{for all } t\ . \tag{131}$$

The approximation $y_1(t)$ is periodic in t with period $1/\Delta$. It can be expressed exactly as

$$y_1(t) = \int df\ \exp(i2\pi ft)\ Y(f)\ \Delta\ \delta_\Delta(f) = \tag{132}$$

$$= y(t) \oplus \delta_{1/\Delta}(t) = \sum_n y\left(t - \frac{n}{\Delta}\right) \quad \text{for all } t\ . \tag{133}$$

That is, approximation $y_1(t)$ is an aliased version of desired waveform y(t), with displacements $1/\Delta$ in time. This result holds for any complex waveform y(t) and has been used repeatedly in the analyses above.

The second approximation of interest is obtained from the cosine transform in (125), which applies for causal complex y(t) in the form

$$y_{2c}(t) \equiv 2\Delta \sum_n \cos(2\pi n\Delta t)\ Y(n\Delta) \quad \text{for all } t\ . \tag{134}$$

$y_{2c}(t)$ also has period $1/\Delta$ in t and can be developed as follows:

$$y_{2c}(t) = \Delta \sum_n [\exp(i2\pi n\Delta t) + \exp(-i2\pi n\Delta t)]\, Y(n\Delta) =$$

$$= \int df\, [\exp(i2\pi ft) + \exp(-i2\pi ft)]\, Y(f)\, \Delta\, \delta_\Delta(f) =$$

$$= [y(t) + y(-t)] \oplus \delta_{1/\Delta}(t) = 2\, y_e(t) \oplus \delta_{1/\Delta}(t) =$$

$$= \sum_n \left[y\left(t - \frac{n}{\Delta}\right) + y\left(\frac{n}{\Delta} - t\right) \right] \quad \text{for all } t\ . \tag{135}$$

That is, sampling of the cosine transform in (125) results in aliasing of y(t) plus its mirror image y(-t), even when y(t) is causal. This will restrict useful results in $y_{2c}(t)$ to a region approximately half as large as that given by (131) and (133), where the sampled exponential transform was used. Even when we restrict calculation of approximation $y_{2c}(t)$ to the region $(0,1/\Delta)$, we are contaminated by the mirror image lobe $y(1/\Delta - t)$ and by the usual lobe $y(t + 1/\Delta)$ extending from $t = -1/\Delta$ into the desired region.

A similar situation exists for using a sampled version of the sine transform for causal complex y(t) in (126); namely, consider the approximation

$$y_{2s}(t) \equiv i2\Delta \sum_n \sin(2\pi n\Delta t)\, Y(n\Delta) \quad \text{for all } t\ . \tag{136}$$

Then

$$y_{2s}(t) = \Delta \sum_n [\exp(i2\pi n\Delta t) - \exp(-i2\pi n\Delta t)]\, Y(n\Delta) =$$

$$= \int df\, [\exp(i2\pi ft) - \exp(-i2\pi ft)]\, Y(f)\, \Delta\, \delta_\Delta(f) =$$

$$= [y(t) - y(-t)] \oplus \delta_{1/\Delta}(t) = 2\, y_o(t) \oplus \delta_{1/\Delta}(t) =$$

$$= \sum_n \left[y\left(t - \frac{n}{\Delta}\right) - y\left(\frac{n}{\Delta} - t\right) \right] \quad \text{for all } t\ . \qquad (137)$$

Here, for the approximate sine transform, twice the odd part of causal complex $y(t)$ is aliased with separations $1/\Delta$ in time, thereby again leading to a clear region only about half that attainable from (131) and (133). We will return to these apparently undesirable transform properties below and find them useful when we consider a causal <u>real</u> time function.

The next approximation is for the noncausal real waveform result in (127); namely, letting $\varepsilon_o = \frac{1}{2}$ and $\varepsilon_n = 1$ for $n \geq 1$, we have trapezoidal approximation

$$y_3(t) \equiv 2\ \mathrm{Re}\ \Delta \sum_{n=0}^{\infty} \varepsilon_n \exp(i2\pi n\Delta t)\, Y(n\Delta) \quad \text{for all } t\ . \qquad (138)$$

Then

$$y_3(t) = 2\ \mathrm{Re} \int_0^{\infty} df\, \exp(i2\pi ft)\, Y(f)\, \Delta\, \delta_\Delta(f) =$$

$$= \int df\, \exp(i2\pi ft)\, Y(f)\, \Delta\, \delta_\Delta(f) = \sum_n y\left(t - \frac{n}{\Delta}\right) \quad \text{for all } t\ , \qquad (139)$$

just as in (133). Thus, the combination of the cosine and sine transforms in (128) does not additionally damage the aliasing behavior associated with sampling. In practice, we would use the real part of the exponential transform as given by (127). The same result, (139), follows when the cosine and sine transforms in (128) are individually directly approximated by the trapezoidal rule and the results added together.

The two final approximations of interest come from sampling the results for causal real y(t) in (129) and (130); from (129), define approximation

$$y_{4c}(t) \equiv 4\Delta \sum_{n=0}^{\infty}{}' \varepsilon_n \cos(2\pi n\Delta t)\, Y_r(n\Delta) \quad \text{for all } t\,, \qquad (140)$$

which has period $1/\Delta$ in t. Now we develop (140) as

$$y_{4c}(t) = 2\Delta \sum_{n} \cos(2\pi n\Delta t)\, Y_r(n\Delta) =$$

$$= 2 \int df \cos(2\pi ft)\, Y_r(f)\, \Delta\, \delta_\Delta(f) =$$

$$= 2 \int df \exp(i2\pi ft)\, Y_r(f)\, \Delta\, \delta_\Delta(f) =$$

$$= \int df \exp(i2\pi ft)\, [Y(f) + Y^*(f)]\, \Delta\, \delta_\Delta(f) =$$

$$= y(t) \oplus \delta_{1/\Delta}(t) + y^*(-t) \oplus \delta_{1/\Delta}(t) =$$

$$= \sum_n y\left(t - \frac{n}{\Delta}\right) + \sum_n y\left(\frac{n}{\Delta} - t\right) = 2\, y_e(t) \oplus \delta_{1/\Delta}(t) \quad \text{for all } t, \qquad (141)$$

where we used the real character of y(t).

This end result is identical to (135); however, approximation $y_{4c}(t)$ in (140) uses only the real part $Y_r(f)$ of the complex function Y(f), whereas $y_{2c}(t)$ in (134) requires the complete complex function Y(f) for a causal complex y(t). Since it is possible to have complex functions Y(f) which have rapidly decaying real parts and slower decaying imaginary parts, (140) affords the possibility of getting a smaller truncation error than (134), when y(t) is causal real and when both sums are carried out to the same frequency limit, because both sums must be terminated in practice. Whether the reduction in the usable "alias-free" region, dictated by (141), can be traded off against a smaller truncation error associated with use of only the real part $Y_r(f)$ in (140), depends on the particular example under investigation. In any event, (140) affords an alternative to consider for causal real y(t).

The final approximation comes about by sampling (130):

$$y_{4s}(t) \equiv -4\Delta \sum_{n=1}^{\infty} \sin(2\pi n\Delta t)\, Y_i(n\Delta) \quad \text{for all } t\ , \qquad (142)$$

which has period $1/\Delta$ in t. In the usual fashion, we find

$$y_{4s}(t) = -2\Delta \sum_n \sin(2\pi n\Delta t)\ Y_i(n\Delta) =$$

$$= -2 \int df\ \sin(2\pi ft)\ Y_i(f)\ \Delta\ \delta_\Delta(f) =$$

$$= i2 \int df\ \exp(i2\pi ft)\ Y_i(f)\ \Delta\ \delta_\Delta(f) =$$

$$= \int df\ \exp(i2\pi ft)\ [Y(f) - Y^*(f)]\ \Delta\ \delta_\Delta(f) =$$

$$= y(t) \oplus \delta_{1/\Delta}(t) - y^*(-t) \oplus \delta_{1/\Delta}(t) = 2\ y_o(t) \oplus \delta_{1/\Delta}(t) =$$

$$= \sum_n y\left(t - \frac{n}{\Delta}\right) - \sum_n y\left(\frac{n}{\Delta} - t\right) \quad \text{for all } t\ . \qquad (143)$$

Here, we used the real character of y(t).

The end result in (143) is identical to (137); however, $y_{4s}(t)$ in (142) only requires knowledge of the imaginary part $Y_i(f)$ of complex function Y(f), whereas $y_{2s}(t)$ in (136) requires the complete complex function Y(f) for a causal complex y(t). This is due to the fact that (129) and (130) apply only to causal real y(t), whereas (125) and (126) apply to causal complex y(t). Since there exist complex functions Y(f) which have more rapidly decaying imaginary parts than real parts, the opportunity arises to reduce the truncation error by employing (142) instead of (136), when y(t) is causal and real. The comments in the sequel to (141), regarding the trade-off between truncation error and a reduced alias-free region, are again applicable.

This procedure, of using only the imaginary part of a Fourier transform because it decays faster than the real part, was utilized to advantage in [4; pages 4 - 6] and was based upon an earlier result in [5; (15)]. The very rapid decay of the imaginary part far outweighed the aliasing; see [4; page 6].

EVALUATION BY MEANS OF FFTs

If periodic function $y_1(t)$ in (131) is evaluated at the equally spaced time points $k/(N\Delta)$ for k=0 to N-1, which suffice to cover one period, we obtain

$$y_1\left(\frac{k}{N\Delta}\right) = \Delta \sum_n \exp(i2\pi nk/N)\ Y(n\Delta) = \tag{144}$$

$$= \Delta \sum_{n=0}^{N-1} \exp(i2\pi nk/N)\ z_n\ , \tag{145}$$

where $\{z_n\}$, $0 \le n \le N-1$, is the collapsed version of sequence $\{Y(n\Delta)\}$, $-\infty < n < \infty$. No approximations are involved in this collapsing procedure from (144) to (145). Relation (145) can be accomplished by means of an N-point FFT if N is highly composite.

In a similar fashion, (140) yields samples of the cosine transform as

$$y_{4c}\left(\frac{k}{N\Delta}\right) = 4\Delta \sum_{n=0}^{\infty} \varepsilon_n \cos(2\pi nk/N)\ Y_r(n\Delta) =$$

$$= 4\Delta\ \mathrm{Re} \sum_{n=0}^{\infty} \exp(i2\pi nk/N)\ \varepsilon_n\ Y_r(n\Delta) = \tag{146}$$

$$= 4\Delta\ \mathrm{Re} \sum_{n=0}^{N-1} \exp(i2\pi nk/N)\ z_n\ , \tag{147}$$

where $\{z_n\}$, $0 \le n \le N-1$, is the collapsed version of sequence $\{\varepsilon_n\ Y_r(n\Delta)\}$, $0 \le n < \infty$.

Since (147) will likely be realized as the real part of an FFT output, the question arises as to the interpretation and utility of the total complex FFT output in (147). To this aim, we rewrite $y_{4c}(t)$ in (146) (in its continuous time version) as

$$y_{4c}(t) = \mathrm{Re}\ 4 \int_0^{\infty} df\ \exp(i2\pi ft)\ Y_r(f)\ \Delta\ \delta_{\Delta}(f) =$$

$$= \mathrm{Re}\{z_1(t) \oplus \delta_{1/\Delta}(t)\}\ , \tag{148}$$

where we define, for all t, Fourier transform

$$z_1(t) = 4 \int_0^{\infty} df\ \exp(i2\pi ft)\ Y_r(f) =$$

$$= \int_0^{\infty} df\ \exp(i2\pi ft)\ [2Y(f) + 2Y^*(f)] =$$

$$= y_+(t) + y_+^*(-t) = [\underline{y}(t) + \underline{y}^*(-t)]\ \exp(i2\pi f_c t) =$$

$$= y(t) + y(-t) + i[y_H(t) - y_H(-t)]\ . \tag{149}$$

That is, $y_{4c}(t)$ is the real part of the aliased version of $z_1(t)$, which itself is composed of the analytic waveform $y_+(t)$ and its mirror image. Thus, not only is $z_1(t)$ aliased according to (148), but in addition, $z_1(t)$ contains terms which will further overlap and thereby confuse the values of $y_{4c}(t)$ in the fundamental range $(0,1/\Delta)$. (Of course, the real part of $z_1(t)$ in (149) for $t > 0$ is, as expected, just $y(t)$ for this causal real case.)

Finally, sampling the sine transform of $Y_i(f)$ in (142) yields

$$y_{4s}\left(\frac{k}{N\Delta}\right) = -4\Delta \sum_{n=1}^{\infty} \sin(2\pi nk/N)\, Y_i(n\Delta) =$$

$$= -4\Delta\, \mathrm{Im} \sum_{n=1}^{\infty} \exp(i2\pi nk/N)\, Y_i(n\Delta) = \qquad (150)$$

$$= -4\Delta\, \mathrm{Im} \sum_{n=0}^{N-1} \exp(i2\pi nk/N)\, z_n\ , \qquad (151)$$

where $\{z_n\}$, $0 \le n \le N-1$, is the collapsed version of sequence $\{Y_i(n\Delta\}$, $1 \le n < \infty$. Relation (151) can be realized as an N-point FFT of which only the imaginary part is kept for $0 \le k \le N-1$.

As above, the interpretation of the complete complex output of the FFT in (151) is furnished by returning to the continuous version of the sampled $y_{4s}(t)$ in (150). We express it as

$$y_{4s}(t) = -\,\mathrm{Im}\; 4 \int_0^{\infty} df\, \exp(i2\pi ft)\, Y_i(f)\, \Delta\, \delta_\Delta(f) =$$

$$= \mathrm{Im}\{z_2(t) \oplus \delta_{1/\Delta}(t)\}\ , \qquad (152)$$

where we define, for all t, Fourier transform

$$z_2(t) = -4 \int_0^\infty df \exp(i2\pi ft)\, Y_i(f) =$$

$$= i \int_0^\infty df \exp(i2\pi ft)\, [2Y(f) - 2Y^*(f)] =$$

$$= i[y_+(t) - y_+^*(-t)] = i[\underline{y}(t) - \underline{y}^*(-t)] \exp(i2\pi f_c t) = \quad (153)$$

$$= i[y(t) - y(-t)] - y_H(t) - y_H(-t)\ . \quad (154)$$

Again, the aliasing of $z_2(t)$ in (152) and the mirror image of the analytic waveform and complex envelope in (153) will serve to confuse the usefulness of $z_2(t)$. The imaginary part of $z_2(t)$ in (154) for $t > 0$ is just $y(t)$, as expected, for this causal real waveform.

DISPLACED SAMPLING

If displaced samples of a waveform are desired, such as at time locations $(k+\beta)/(N\Delta)$ in (145), where $0 < \beta < 1$, we can obtain them via an N-point FFT as follows: from (131),

$$y_1\left(\frac{k+\beta}{N\Delta}\right) = \Delta \sum_n \exp(i2\pi nk/N)\ \exp(i2\pi n\beta/N)\ Y(n\Delta) = \qquad (155)$$

$$= \Delta \sum_{n=0}^{N-1} \exp(i2\pi nk/N)\ z_n \quad \text{for } 0 \le k \le N-1\ , \qquad (156)$$

where $\{z_n\}$, $0 \le n \le N-1$, is the collapsed version of sequence $\{\exp(i2\pi n\beta/N)\ Y(n\Delta)\}$, $-\infty < n < \infty$. That is, we have to load up the arrays containing $\{z_n\}$ with phase-shifted versions of the original sequence $\{Y(n\Delta)\}$ and then perform the N-point FFT. Calculation of phasor $p_n = \exp(i2\pi n\beta/N)$ in (155) can take advantage of recursion $p_n = p_{n-1}\ \exp(i2\pi\beta/N)$.

SUMMARY

The advantages of filtering the complex envelope spectrum by means of a suitable lowpass filter are significant in some instances. The singular behavior of the complex envelope waveform is eliminated by utilizing a filter which cuts off at finite frequencies, while the slow decay in the time domain of the complex envelope is circumvented by using a filter with a smoothly tapered cutoff that prevents any discontinuities in the complex envelope spectrum from contributing.

The use of an FFT to evaluate the filtered complex envelope is then an attractive efficient approach because the inherent time aliasing associated with frequency sampling has been greatly suppressed. Also, the very rapidly varying singular components of the complex envelope have been eliminated, allowing for a lower time-sampling rate, that is, smaller FFT sizes.

When two waveforms, each with its own imposed amplitude- and phase-modulations, are convolved, such as encountered in the narrowband excitation of a passband filter, the output complex envelope is given exactly by the convolution of the individual complex envelopes. Although the convolution of the two (complex) imposed modulations is often a good approximation to the output complex envelope, it has an error term. This analysis is presented in appendix C.

APPENDIX A. DETERMINATION OF CENTER FREQUENCY

Suppose we are given spectrum Y(f) of (narrowband) real waveform y(t), but the center frequency of Y(f) is not obvious or is unknown. The analytic waveform is still uniquely given by

$$y_+(t) = \int df\ \exp(i2\pi ft)\ Y_+(f) = 2 \int_0^\infty df\ \exp(i2\pi ft)\ Y(f)\ . \quad (A\text{-}1)$$

Make a guess at initial frequency f_i near the center of $Y_+(f)$. Then compute the initial down-shifted waveform

$$y_i(t) \equiv \exp(-i2\pi f_i t)\ y_+(t) = 2 \int_{-f_i}^\infty df\ \exp(i2\pi ft)\ Y(f+f_i)\ . \quad (A\text{-}2)$$

Compute initial phase $P_i(t) = \arg\{y_i(t)\}$ and then unwrap $P_i(t)$. Select time t in the interval T of interest and fit a straight line $\alpha + \beta t$ to the unwrapped phase $P_i(t)$ over T. Compute frequency

$$f_c = f_i + \frac{\beta}{2\pi}\ ; \quad (A\text{-}3)$$

this is the center frequency of $y_+(t)$ for $t \in T$. Another selection of a different time interval could lead to a somewhat different center frequency; there is no unique center frequency of an arbitrarily given spectrum Y(f).

The complex envelope is then

$$\underline{y}(t) = \exp(-i2\pi f_c t)\ y_+(t)\ . \quad (A\text{-}4)$$

The "physical" envelope or extracted amplitude modulation is

$$A(t) = |\underline{y}(t)| = |y_+(t)| = |y_i(t)| \ , \qquad \text{(A-5)}$$

which is independent of the choice of f_i or f_c. The extracted phase of complex envelope $\underline{y}(t)$ is

$$P(t) = \arg\{\underline{y}(t)\} = \arg\{y_+(t)\ \exp(-i2\pi f_c t)\} = P_i(t) - \beta t \ , \qquad \text{(A-6)}$$

where we used (A-4) and (A-2). Functions $y_i(t)$ and $P_i(t)$ have already been computed and can be used to evaluate the envelope $A(t)$ and phase $P(t)$. The real waveform is

$$y(t) = \text{Re}\{y_+(t)\} = \text{Re}\{\underline{y}(t)\ \exp(i2\pi f_c t)\} = A(t)\ \cos[2\pi f_c t + P(t)], \qquad \text{(A-7)}$$

in terms of chosen center frequency f_c and amplitude and phase modulations $A(t)$ and $P(t)$, respectively. Although f_c and $P(t)$ are not unique, the argument of the cosine and the waveform $y(t)$ in (A-7) are unique, as may be seen by the first equality in (A-7). All of these relations hold for time $t \in T$.

If the fit of the straight line $\alpha + \beta t$ to initial unwrapped phase $P_i(t)$ over interval T is via minimum error energy, then we find

$$\beta = \frac{\mu_o \nu_1 - \mu_1 \nu_o}{\mu_o \mu_2 - \mu_1^2} \ , \qquad \mu_n = \int_T dt\ t^n \ , \qquad \nu_n = \int_T dt\ t^n\ P_i(t) \ . \qquad \text{(A-8)}$$

There is no need to explicitly compute α, although it should be included in the error energy minimization in order to afford a better fit.

APPENDIX B. PROGRAM FOR FILTERED COMPLEX ENVELOPE VIA FFT

The program listed below actually computes the unfiltered complex envelope by means of an FFT. In order to convert it to one which will compute the filtered complex envelope, remove lines 220 - 320 and replace them by the following lines:

```
220    F1=40.                 !  CUTOFF FREQUENCY < Fo
230    H1=.5*PI/F1
240    M1=M*F1/Fo
250    FOR Ms=-M1 TO M1       !  -F1 < F < F1
260    J=Ms MODULO N          !  COLLAPSING
270    F=Df*Ms                !  FREQUENCY f
280    CALL Y(F+Fo,Al,Wo,Cp,Sp,Yr,Yi) !SHIFTED FREQUENCY FUNCTION
290    Cos=COS(H1*F)
300    H=Cos*Cos              !  REAL LOWPASS HANN FILTER
310    X(J)=X(J)+Yr*H
320    Y(J)=Y(J)-Yi*H         !  CONJUGATE INPUT INTO FFT
```

```
 10  ! COMPLEX ENVELOPE VIA SHIFTED FREQUENCY FUNCTION
 20    Al=1                   !  DAMPING ALPHA
 30    Fo=100                 !  CARRIER FREQUENCY
 40    Phi=-PI/2              !  PHASE
 50    M=8000                 !  NUMBER OF SAMPLES FOR F < 0; LINE 270
 60    N=1024                 !  SIZE OF FFT; ZERO SUBSCRIPT
 70    REDIM Cos(0:N/4),X(0:N-1),Y(0:N-1)
 80    DIM Cos(1024),X(4096),Y(4096)
 90    DOUBLE M,N,N2,J,Ms     !  INTEGERS, NOT DOUBLE PRECISION
100    N2=N/2
110    A=2.*PI/N
120    FOR J=0 TO N/4
130    Cos(J)=COS(A*J)        !  QUARTER-COSINE TABLE IN Cos(*)
140    NEXT J
150    Cp=COS(Phi)
160    Sp=SIN(Phi)
170    Wo=2*PI*Fo
180    Df=Fo/M                !  FREQUENCY INCREMENT
190    Dt=1./(N*Df)           !  TIME INCREMENT ON COMPLEX ENVELOPE
200    MAT X=(0.)
210    MAT Y=(0.)
220    Ms=-M
230    J=Ms MODULO N
240    CALL Y(0.,Al,Wo,Cp,Sp,Yr,Yi)  !  Y(0)
250    X(J)=.5*Yr
260    Y(J)=-.5*Yi            !  CONJUGATE INPUT TO FFT
270    FOR Ms=-M+1 TO M*10    !  NOTICE UPPER LIMIT ON FREQUENCY
280    J=Ms MODULO N          !  COLLAPSING
290    F=Df*Ms                !  FREQUENCY f
300    CALL Y(F+Fo,Al,Wo,Cp,Sp,Yr,Yi)  !  SHIFTED FREQUENCY FUNCTION
310    X(J)=X(J)+Yr
320    Y(J)=Y(J)-Yi           !  CONJUGATE INPUT TO FFT
330    NEXT Ms
```

```
340     MAT X=X*(2.*Df)
350     MAT Y=Y*(2.*Df)                    !   *       CONJUGATE
360     CALL Fft14(N,Cos(*),X(*),Y(*))     !  y (t)    OF COMPLEX
370     GINIT                              !  -        ENVELOPE
380     PLOTTER IS "GRAPHICS"
390     GRAPHICS ON
400     WINDOW -N2,N2,-8,0                 !  CENTER PLOT AT TIME t = 0
410     LINE TYPE 3
420     GRID N/8,1
430     LINE TYPE 4
440     MOVE 0,0
450     Ts=Dt*N/4
460     DRAW N/4,LGT(EXP(-A1*Ts))
470     PENUP
480     LINE TYPE 1
490     FOR Ms=-N2 TO N2
500     J=Ms MODULO N
510     X=X(J)
520     Y=Y(J)
530     T=X*X+Y*Y              !  MAGNITUDE SQUARED COMPLEX ENVELOPE
540     IF T>0. THEN 570
550     PENUP
560     GOTO 580
570     PLOT Ms,LGT(T)*.5      !  MAGNITUDE OF COMPLEX ENVELOPE
580     NEXT Ms
590     PENUP
600     PAUSE
610     GCLEAR
620     GRAPHICS ON
630     WINDOW -N2,N2,-PI,PI
640     LINE TYPE 3
650     GRID N/8,PI/2
660     LINE TYPE 1
670     FOR Ms=-N2 TO N2           !  PLOT COMPLEX ENVELOPE PHASE
680     J=Ms MODULO N
690     PLOT Ms,FNArg(X(J),-Y(J))  !  CONJUGATE THE FFT OUTPUT
700     NEXT Ms
710     PENUP
720     PAUSE
730     GCLEAR
740     GRAPHICS ON
750     LINE TYPE 3
760     GRID N/8,PI/2
770     LINE TYPE 1
780     FOR Ms=-N2 TO N2
790     J=Ms MODULO N
800     Ts=Ms*Dt               !  TIME t
810     Cos=COS(Wo*Ts)         !  SHIFT PHASE THE
820     Sin=SIN(Wo*Ts)         !  COMPLEX ENVELOPE BY Wo Ts
830     X=X(J)
840     Y=-Y(J)                !  CONJUGATE THE FFT OUTPUT
850     PLOT Ms,FNArg(X*Cos-Y*Sin,X*Sin+Y*Cos)
860     NEXT Ms
870     PENUP
880     PAUSE
890     END
900     !
```

```
 910    DEF FNArg(X,Y)       !  PRINCIPAL ARG(Z)
 920    IF X=0. THEN RETURN .5*PI*SGN(Y)
 930    A=ATN(Y/X)
 940    IF X>0. THEN RETURN A
 950    IF Y<0. THEN RETURN A-PI
 960    RETURN A+PI
 970    FNEND
 980    !
 990    SUB Y(F,A1,Wo,Cp,Sp,Yr,Yi)  !  SPECTRAL FUNCTION
1000    W=2.*PI*F
1010    T=W-Wo
1020    D=A1*A1+T*T
1030    R1=(Cp*A1+Sp*T)/D
1040    I1=(Sp*A1-Cp*T)/D
1050    T=W+Wo
1060    D=A1*A1+T*T
1070    R2=(Cp*A1-Sp*T)/D
1080    I2=(-Sp*A1-Cp*T)/D
1090    Yr=.5*(R1+R2)
1100    Yi=.5*(I1+I2)
1110    SUBEND
1120    !
1130    SUB Fft14(DOUBLE N,REAL Cos(*),X(*),Y(*)) ! N<=2^14=16384; 0 SUBS
1140    DOUBLE Log2n,N1,N2,N3,N4,J,K   !  INTEGERS < 2^31 = 2,147,483,648
1150    DOUBLE I1,I2,I3,I4,I5,I6,I7,I8,I9,I10,I11,I12,I13,I14,L(0:13)
1160    IF N=1 THEN SUBEXIT
1170    IF N>2 THEN 1250
1180    A=X(0)+X(1)
1190    X(1)=X(0)-X(1)
1200    X(0)=A
1210    A=Y(0)+Y(1)
1220    Y(1)=Y(0)-Y(1)
1230    Y(0)=A
1240    SUBEXIT
1250    A=LOG(N)/LOG(2.)
1260    Log2n=A
1270    IF ABS(A-Log2n)<1.E-8 THEN 1300
1280    PRINT "N =";N;"IS NOT A POWER OF 2; DISALLOWED."
1290    PAUSE
1300    N1=N/4
1310    N2=N1+1
1320    N3=N2+1
1330    N4=N3+N1
1340    FOR I1=1 TO Log2n
1350    I2=2^(Log2n-I1)
1360    I3=2*I2
1370    I4=N/I3
1380    FOR I5=1 TO I2
1390    I6=(I5-1)*I4+1
1400    IF I6<=N2 THEN 1440
1410    A1=-Cos(N4-I6-1)
1420    A2=-Cos(I6-N1-1)
1430    GOTO 1460
1440    A1=Cos(I6-1)
1450    A2=-Cos(N3-I6-1)
1460    FOR I7=0 TO N-I3 STEP I3
1470    I8=I7+I5-1
1480    I9=I8+I2
```

```
1490    T1=X(I8)
1500    T2=X(I9)
1510    T3=Y(I8)
1520    T4=Y(I9)
1530    A3=T1-T2
1540    A4=T3-T4
1550    X(I8)=T1+T2
1560    Y(I8)=T3+T4
1570    X(I9)=A1*A3-A2*A4
1580    Y(I9)=A1*A4+A2*A3
1590    NEXT I7
1600    NEXT I5
1610    NEXT I1
1620    I1=Log2n+1
1630    FOR I2=1 TO 14
1640    L(I2-1)=1
1650    IF I2>Log2n THEN 1670
1660    L(I2-1)=2^(I1-I2)
1670    NEXT I2
1680    K=0
1690    FOR I1=1 TO L(13)
1700    FOR I2=I1 TO L(12) STEP L(13)
1710    FOR I3=I2 TO L(11) STEP L(12)
1720    FOR I4=I3 TO L(10) STEP L(11)
1730    FOR I5=I4 TO L(9) STEP L(10)
1740    FOR I6=I5 TO L(8) STEP L(9)
1750    FOR I7=I6 TO L(7) STEP L(8)
1760    FOR I8=I7 TO L(6) STEP L(7)
1770    FOR I9=I8 TO L(5) STEP L(6)
1780    FOR I10=I9 TO L(4) STEP L(5)
1790    FOR I11=I10 TO L(3) STEP L(4)
1800    FOR I12=I11 TO L(2) STEP L(3)
1810    FOR I13=I12 TO L(1) STEP L(2)
1820    FOR I14=I13 TO L(0) STEP L(1)
1830    J=I14-1
1840    IF K>J THEN 1910
1850    A=X(K)
1860    X(K)=X(J)
1870    X(J)=A
1880    A=Y(K)
1890    Y(K)=Y(J)
1900    Y(J)=A
1910    K=K+1
1920    NEXT I14
1930    NEXT I13
1940    NEXT I12
1950    NEXT I11
1960    NEXT I10
1970    NEXT I9
1980    NEXT I8
1990    NEXT I7
2000    NEXT I6
2010    NEXT I5
2020    NEXT I4
2030    NEXT I3
2040    NEXT I2
2050    NEXT I1
2060    SUBEND
```

APPENDIX C. CONVOLUTION OF TWO WAVEFORMS

Suppose real waveform x(t) excites passband filter H(f) with real impulse response h(t). Then, the output is

$$Y(f) = H(f)\ X(f)\ , \qquad y(t) = h(t) \oplus x(t)\ . \tag{C-1}$$

The single-sided output spectrum is

$$Y_+(f) = 2\ U(f)\ Y(f) = 2\ U(f)\ H(f)\ X(f) = \frac{1}{2}\ H_+(f)\ X_+(f)\ . \tag{C-2}$$

The corresponding output analytic waveform is exactly

$$y_+(t) = \frac{1}{2}\ h_+(t) \oplus x_+(t)\ , \tag{C-3}$$

which is just (one-half of) the convolution of the individual analytic waveforms.

If the center frequency of $Y_+(f)$ is f_c (see appendix A), then the spectrum of the output complex envelope is, using (C-2),

$$\underline{Y}(f) = Y_+(f+f_c) = \frac{1}{2}\ H_+(f+f_c)\ X_+(f+f_c) = \frac{1}{2}\ \underline{H}(f)\ \underline{X}(f)\ , \tag{C-4}$$

where we have taken the <u>same</u> center frequency, f_c, for $H_+(f)$ as well as $X_+(f)$. This relation in (C-4) is exact; it involves <u>no narrowband approximations</u>. The output complex envelope corresponding to (C-4) is then exactly

$$\underline{y}(t) = \frac{1}{2}\ \underline{h}(t) \oplus \underline{x}(t)\ . \tag{C-5}$$

That is, the complex envelope of the convolution of any two waveforms is equal to (one-half of) the convolution of the two individual complex envelopes, irrespective of their frequency

contents.

Now suppose that x(t) is given in terms of some complex imposed modulation $x_i(t)$ according to

$$x(t) = \mathrm{Re}\{x_i(t)\ \exp(i2\pi f_c t)\}\ , \qquad \text{(C-6)}$$

which allows for amplitude-modulation as well as phase-modulation. The spectrum of x(t) can then be expressed as

$$X(f) = \frac{1}{2}\ [X_i(f-f_c) + X_i^*(-f-f_c)]\ . \qquad \text{(C-7)}$$

Also, suppose that filter impulse response h(t) is expressible in a similar form according to

$$h(t) = \mathrm{Re}\{h_i(t)\ \exp(i2\pi f_c t)\}\ , \qquad \text{(C-8)}$$

with corresponding transfer function

$$H(f) = \frac{1}{2}\ [H_i(f-f_c) + H_i^*(-f-f_c)]\ . \qquad \text{(C-9)}$$

The filter output spectrum then follows from (C-1), (C-7), and (C-9) as

$$Y(f) = \frac{1}{4}\ [H_i(f-f_c)\ X_i(f-f_c) + H_i^*(-f-f_c)\ X_i^*(-f-f_c) +$$

$$+ H_i^*(-f-f_c)\ X_i(f-f_c) + H_i(f-f_c)\ X_i^*(-f-f_c)\ ]\ . \qquad \text{(C-10)}$$

By inverse Fourier transforming the individual terms, the corresponding waveform to (C-10) is found to be exactly

$$y(t) = \mathrm{Re}\{\exp(i2\pi f_c t)\ [y_a(t) + y_b(t)]\}\ , \qquad \text{(C-11)}$$

where

$$y_a(t) = \frac{1}{2}\, h_i(t) \oplus x_i(t) \ , \qquad \text{(C-12)}$$

and

$$y_b(t) = \frac{1}{2}\, [h_i^*(t)\, \exp(-i4\pi f_c t)] \oplus x_i(t) \ . \qquad \text{(C-13)}$$

Relation (C-12) states that component $y_a(t)$ of output $y(t)$ in (C-11) is just the convolution of the two complex imposed modulations $h_i(t)$ and $x_i(t)$. However, (C-11) and (C-13) reveal that there is an additional term in $y(t)$, which requires the convolution of a relatively high-frequency component, namely $\exp(-i4\pi f_c t)$. Since this latter term, $y_b(t)$, will often be small due to this oscillatory integrand, we may neglect it in many circumstances.

A good way of assessing the importance of the $y_b(t)$ term in (C-11) is to observe that it is due to the second line of the spectrum in (C-10); the first line in (C-10) corresponds to $y_a(t)$. Since $H_i(f)$ and $X_i(f)$ are generally lowpass functions of frequency, the function $H_i(-f-f_c)$ in (C-10) is centered around $f = -f_c$, while the $X_i(f-f_c)$ term peaks near $f = f_c$. The separation of these two functions is approximately $2f_c$ on the f axis; if this separation is somewhat greater than the bandwidths of H_i and X_i, then there is inconsequential overlap of any of the frequency components in the second line of (C-10). This leads to a small value for $y_b(t)$ for all t and we can neglect its effect relative to $y_a(t)$ in (C-11).

REFERENCES

[1] A. H. Nuttall, **Alias-Free Wigner Distribution Function and Complex Ambiguity Function for Discrete-Time Samples,** NUSC Technical Report 8533, Naval Underwater Systems Center, New London, CT, 14 April 1989.

[2] A. H. Nuttall, "On the Quadrature Approximation to the Hilbert Transform of Modulated Signals", **Proceedings IEEE,** volume 54, number 10, pages 1458 - 1459, October 1966.

[3] **Handbook of Mathematical Functions,** U. S. Department of Commerce, National Bureau of Standards, Applied Mathematics Series, Number 55, U. S. Government Printing Office, Washington, DC, June 1964.

[4] A. H. Nuttall and B. Dedreux, **Exact Operating Characteristics for Linear Sum of Envelopes of Narrowband Gaussian Process and Sinewave,** NUSC Technical Report 7117, Naval Underwater Systems Center, New London, CT, 11 January 1984.

[5] A. H. Nuttall, "Alternative Forms and Computational Considerations for Numerical Evaluation of Cumulative Probability Distributions Directly From Characteristic Functions," **Proceedings IEEE,** Volume 58, Number 11, pages 1872 - 1873, November 1970. Also in NUSC Report Number NL-3012, Naval Underwater Systems Center, New London, CT, 12 August 1970.

Reverse Blank

INITIAL DISTRIBUTION LIST

Addressee	No. of Copies
Admiralty Underwater Weapons Establishment, England	
Library	1
Center for Naval Analyses	1
Coast Guard Academy	
Prof. J. J. Wolcin	1
David Taylor Research Center, Bethesda, MD	
Commander	1
H. Chaplin	1
L. Becker	1
W. Phillips (Code 1932)	1
David Taylor Research Center, Annapolis	
P. Prendergast (Code 2744)	1
Defense Nuclear Agency, RAAE	
J. Meyers	1
Defence Research Center, Australia	
Library	1
Defence Research Establishment Atlantic, Nova Scotia	
B. E. Mackey (Library)	1
Defence Research Establishment Pacific, British Columbia	
Dr. D. J. Thomson	1
Defence Science Establishment, HMNZ Dockyard, New Zealand	
Director	1
Defence Scientific Establishment, New Zealand	
Dr. L. H. Hall	1
Defense Advanced Research Projects Agency	
Commanding Officer	1
A. W. Ellinthorpe	1
Defense Intelligence Agency	1
Defense Technical Information Center	12
Dept. of Science & Industrial Research, New Zealand	
M. A. Poletti	1
National Radio Astronomy Observatory	
F. Schwab	1
National Security Agency	
Dr. J. R. Maar (R51)	1
Naval Air Development Center	
Commander	1
A. Witt	1
T. Madera	1
L. Allen (Code 50)	1
Naval Air Systems Command	
NAIR 93	1
Naval Coastal Systems Center	
Commanding Officer	1
D. Skinner	1
E. Linsenmeyer	1
Naval Environmental Prediction Research Facility	1
Naval Intelligence Command	1
Naval Oceanographic Office	1

INITIAL DISTRIBUTION LIST (CONT'D)

Addressee	No. of Copies
Naval Oceanographic & Atmospheric Research Laboratory, CA	
M. J. Pastore	1
Naval Oceanographic & Atmospheric Research Laboratory, MS	
Commanding Officer	1
R. Wagstaff (Code 245)	1
B. Adams	1
E. Franchi	1
R. Fiddler (Code 245)	1
Naval Ocean Systems Center, Hawaii	1
Naval Ocean Systems Center, San Diego	
Commanding Officer	1
J. M. Alsup (Code 635)	1
J. Silva	1
D. Hanna	1
P. Nachtigall	1
W. Marsh	1
C. Persons	1
Naval Personnel Research & Development Center	1
Naval Postgraduate School	
Superintendent	2
Prof. C. W. Therrien (Code 62 TI)	1
Naval Research Laboratory, Orlando, USRD	1
Naval Research Laboratory, Washington	
Commanding Officer	1
Dr. P. B. Abraham (Code 5131)	1
W. F. Gabriel (Code 5370)	1
A. A. Gerlach	1
N. Yen (Code 5130)	1
D. Bradley	1
S. Sachs	1
S. Wolfe	1
D. Steiger	1
E. Wald (Code 5150)	1
Naval Sea Systems Command	
SEA-00; -63; -63D; -63X; -92R; PMS-402	6
Naval Surface Warfare Center	
J. Gray (Code G71)	1
Naval Surface Weapons Center, Dahlgren, VA	
Commander	1
H. Crisp	1
D. Phillips	1
T. Ryczek	1
Naval Surface Weapons Center, White Oak Lab.	1
M. Strippling	1
Naval Surface Weapons Center, Fort Lauderdale	1
Naval Technical Intelligence Center	
Commanding Officer	2
D. Rothenberger	1
Naval Underwater Systems Center, West Palm Beach	
Officer in Charge	1
Dr. R. M. Kennedy (Code 3802)	1

INITIAL DISTRIBUTION LIST (CONT'D)

Addressee	No. of Copies
Naval Weapons Center	1
Norwegian Defence Research Establishment	
Dr. J. Glattetre	1
Office of the Chief of Naval Research, Arlington, VA	
OCNR-00; -10; -11; -12; -13; -20; -21; -22; -23 (3)	11
N. L. Gerr (Code 1111)	1
A. Wood	1
D. Johnson	1
SACLANT Undersea Research Center	
Dr. J. P. Ianniello	1
Dr. S. Stergiopolous	1
Prof. G. Tacconi	1
Library	1
Sonar and Surveillance Group, RANRL, Australia	1
Space & Naval Warfare System Command	
SPAWAR-00; -04; -005; PD-80; PMW-181	5
L. Parrish	1
R. Cockerill	1
U.S. Air Force, Alabama	
Air University Library	1
U.S. Coast Guard Research & Development Center	
Library	1
U.S. Department of Commerce, NTIA/ITS	
Dr. A. D. Spaulding	1
Weapons Systems Research Laboratory, Australia	
HASC	1
HSPC	1
Brown University	
Documents Library	1
Canberra College of Advanced Education	
P. Morgan	1
Concordia University, Quebec	
Prof. J. Krolik	1
Dalhousie University	
Dr. B. Ruddick	1
Drexel University	
Prof. S. B. Kesler	1
Harvard University	
Gordon McKay Library	1
Indian Institute of Technology, India	
Dr. K. M. M. Prabhu	1
Johns Hopkins University, Applied Physics Laboratory	
Director	1
J. C. Stapleton	1
Kansas State University	
Prof. B. Harms	1
Lawrence Livermore National Laboratory	
Director	1
L. C. Ng	1

Addressee	No. of Copies
Los Alamos National Laboratory	1
Marine Biological Laboratory, Woods Hole	1
Marine Physical Laboratory, Scripps	1
Massachusetts Institute of Technology	
Prof. A. B. Baggaroer	1
Barker Engineering Library	1
Northeastern University	
Prof. C. L. Nikias	1
Penn State University, Applied Research Laboratory	
Director	1
F. W. Symons	1
R. Hettche	1
E. Liszka	1
Purdue University	
Prof. N. Srinivasa	1
Royal Military College of Canada	
Prof. Y. T. Chan	1
Rutgers University	
Prof. S. Orfanidis	1
San Diego State University	
Prof. F. J. Harris	1
Sandia National Laboratory	
Director	1
J. Claasen (315)	1
Simon Fraser University	
Dr. E. F. Velez	1
Southeastern Massachusetts University	
Prof. C. H. Chen	1
State University of New York	
Prof. M. Barkat	1
Tel-Aviv University, Israel	
Prof. E. Weinstein	1
United Engineering Center	
Engineering Societies Library	1
University of Alberta, Canada	
K. L. Yeung	1
University of Auckland	
Dr. M. D. Johns	1
University of California, San Diego	
Prof. C. W. Helstrom	1
University of Colorado	
Prof. L. L. Scharf	1
University of Connecticut	
Prof. C. H. Knapp	1
Wilbur Cross Library	1
University of Florida	
Prof. D. C. Childers	1
University of Illinois	
Dr. D. L. Jones	1

Addressee	No. of Copies
University of Michigan	
Communications & Signal Processing Laboratory	1
W. J. Williams	1
University of Minnesota	
Prof. M. Kaveh	1
University of Queensland	
Dr. B. Boashash	1
University of Rhode Island	
Prof. G. F. Boudreaux-Bartels	1
Prof. S. M. Kay	1
Prof. D. Tufts	1
Library	1
University of Rochester	
Prof. E. Titlebaum	1
University of Southern California	
Prof. W. C. Lindsey	1
Dr. A. Polydoros	1
University of Strathclyde, Scotland	
Prof. T. S. Durrani	1
University of Technology, England	
Prof. J. W. R. Griffiths	1
University of Texas, Applied Research Laboratory	1
University of Washington	
Applied Physics Laboratory	1
Prof. D. W. Lytle	1
Dr. R. C. Spindel	1
Villanova University	
Prof. M. G. Amin	1
Woods Hole Oceanographic Institution	
Director	1
Dr. E. Weinstein	1
Yale University	
Prof. A. Nehorai	1
Prof. P. M. Schultheiss	1
Prof. F. Tuteur	1
Kline Science Library	1
Applied Seismic Group	
R. Lacoss	1
A&T, North Stonington, CT	
H. Jarvis	1
A&T, Arlington, VA	
D. L. Clark	1
BB&N, Arlington, VA	
Dr. H. Cox	1
BB&N, Cambridge, MA	
H. Gish	1
BB&N, New London, CT	
Dr. P. G. Cable	1

Addressee	No. of Copies
Bell Communications Research	
J. F. Kaiser	1
D. Sunday	1
Cogent Systems, Inc.	
J. P. Costas	1
Diagnostic/Retrieval Systems, Inc.	
J. Williams	1
EDO Corporation	
M. Blanchard	1
EG&G	
D. Frohman	1
General Electric Company, Moorestown, NJ	
Dr. M. R. Allen	1
H. Urkowitz	1
General Electric Company, Philadelphia, PA	
T. J. McFall	1
General Electric Company, Pittsfield, MA	
R. W. Race	1
General Electric Company, Syracuse, NY	
Dr. A. M. Vural	1
D. Winfield	1
Harris Scientific Services	
B. Harris	1
Hughes Aircraft Company, Buena Park, CA	
T. E. Posch	1
IBM	
G. L. Demuth	1
Interstate Electronics Corporation	
R. O. Nielsen (Dept. 8011)	1
Kildare Corporation	
Dr. R. Mellen	1
Lincom Corporation	
Dr. T. A. Schonhoff	1
Magnavox Elec. Systems Company	
R. Kenefic (Dept. 525)	1
MSB Systems, Inc.	
A. Winder	1
Nichols Research Corporation	
Dr. T. L. Marzetta	1
Orincon Corporation	
S. L. Marple	1
Dr. J. W. Young	1
Prometheus, Inc., Newport, RI	
M. J. Barrett	1
Prometheus, Inc., Sharon, MA	
Dr. J. S. Byrnes	1
RAN Research Lab, Australia	1

Addressee	No. of Copies
Raytheon, Portsmouth, RI	
J. Bartram	1
R. Conner	1
S. S. Reese	1
Rockwell International	
L. T. Einstein	1
Dr. D. F. Elliott	1
SAIC, Falls Church, VA	
Dr. P. Mikhalevsky	1
SAIC, New London	
Dr. F. DiNapoli	1
SIMRAD SUBSEA A/S, Naval Systems Div.	
E. B. Lunde	1
Sperry Corporation, Defense Marine Systems Unit	1
Toyon Research Corporation	
M. L. Van Blaricum	1
Tracor	
Dr. T. J. Leih	1
TRW, Fairfax, VA	
R. Prager	1
G. Maher	1
TRW, New London, CT	
D. Sturim	1
Welse Sistemi Subacquei, Genova, Italy	
Dr. H. Van Asselt	1
Westinghouse Electric Corporation, Annapolis, MD	
H. Newman	1
Dr. H. L. Price	1
Westinghouse Electric Corporation, Baltimore, MD	
R. Park	1
Westinghouse Electric Corporation, Waltham, MA	
R. B. Kennedy	1
Assard, G. L.	1
Beidas, B.	1
Bendat, Dr. J. S.	1
Bleistein, Dr. N.	1
Cohen, Dr. L.	1
Hahn, W. R.	1
Lloyd, L.	1
Maltz, F.	1
Middleton, Dr. D.	1
Nash, H. E.	1
Nicholson, D.	1
O'Brien, W.	1
Papoutsanis, P.D.	1
Pohler, R. F.	1

Addressee	No. of Copies
Price, Dr. R.	1
Raisbeck, Dr. G.	1
Richter, W.	1
Schulkin, Dr. M.	1
Urick, R. J.	1
Von Winkle, Dr. W. A.	1
Werbner, A.	1
Wilson, Dr. J. H.	1